



Weak and Strong Interaction of Excitation Kinks in Scalar Parabolic Equations

Antoine Pauthier¹ · Jens D. M. Rademacher¹ · Dennis Ulbrich¹ 

Received: 30 November 2020 / Revised: 21 June 2021 / Accepted: 29 June 2021 /
Published online: 30 July 2021
© The Author(s) 2021

Abstract

Motivated by studies of the Greenberg-Hastings cellular automata (GHCA) as a caricature of excitable systems, in this paper we study kink-antikink dynamics in the perhaps simplest PDE model of excitable media given by the scalar reaction diffusion-type θ -equations for excitable angular phase dynamics. On the one hand, we qualitatively study geometric kink positions using the comparison principle and the theory of terraces. This yields the minimal initial distance as a global lower bound, a well-defined sequence of collision data for kinks- and antikinks, and implies that periodic pure kink sequences are asymptotically equidistant. On the other hand, we study metastable dynamics of finitely many kinks using weak interaction theory for certain analytic kink positions, which admits a rigorous reduction to ODE. By blow-up type singular rescaling we show that distances become ordered in finite time, and eventually diverge. We conclude that diffusion implies a loss of information on kink distances so that the entropic complexity based on positions and collisions in the GHCA does not simply carry over to the PDE model.

Keywords Scalar parabolic equations · Kink dynamics · Comparison principle

Mathematics Subject Classification 35K55 · 35B05 · 37L25

1 Introduction

Many spatially extended physical, chemical and biological systems form so-called excitable media, in which a supercritical perturbation from a stable equilibrium triggers an excitation that is transferred to its neighbours, followed by refractory return to the rest state.

Perhaps the simplest dynamical system that realises a caricature excitable medium is the 1D Greenberg-Hastings cellular automata (GHCA) [25,26]. Its key features are that spatial

We thank the reviewer for careful reading and helpful comments which improved the manuscript. This work has been supported by Grant RA 2788/1-1 of the German research fund (DFG).

✉ Dennis Ulbrich
d.ulbrich@uni-bremen.de

¹ Department 3: Mathematics, University of Bremen, Bibliothekstr. 5, 28359 Bremen, Germany

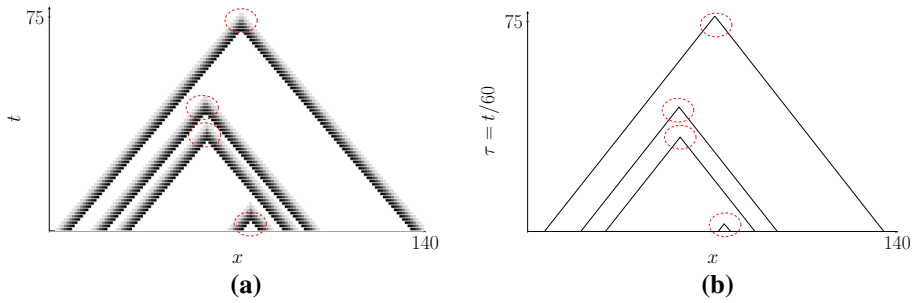


Fig. 1 Space-time plots of pulse positions for GHCA **a** and positions (2) of (1), **b** with $f_0 = 0.05$ for initial data with four pairs of pulses and kinks/antikinks, respectively; marked are the associated annihilation events. In the right panel, time is rescaled such that a single front has unit speed as in the left panel. Some details on the numerics can be found in “Appendix C”

excitation loops embedded between rest states form local pulses that travel in one direction, and a counter-propagating pair of such local pulses annihilates, leading to a pure rest state locally, cf. Fig. 1a. Pulse trains can be generated from local pulses by placing these at arbitrary positions; they will maintain their relative distance until a possible annihilation. In fact, the topological entropy of the GHCA results from a Devaney-chaotic closed invariant subset of the non-wandering set that consists of colliding and annihilating local pulses [16,31]. From a dynamical systems viewpoint the non-wandering set is of prime relevance, and it turns out that for the GHCA it can be decomposed into invariant sets with different wave dynamics [31].

However, the modelling of excitable media is predominantly done by parabolic partial differential equations (PDE) and systems thereof. A paradigm is the famous FitzHugh-Nagumo (FHN) equation, derived from the Hodgkin-Huxley model for nerve axons [19,27,37]. A priori, for any such PDE model, the identification and description of pulse dynamics akin to GHCA is a formidable task and far from completely understood even in FHN. The PDE dynamics is in general also richer and parameter dependent, for instance self-replication of pulses has been numerically observed [11,28], and rebound of pulses upon collision [38].

In nature and experiments, one can effectively find both, discrete and continuous excitable media. As basic examples one may consider, for a discrete situation, a set of neurons that is spatially arranged in the cortex, and, for a paradigm of a continuous medium, a Petri dish with the fluid mixture for the Belousov-Zhabotinsky reaction. Although the spatio-temporal propagation of excitations structurally differ, characteristic propagating waves can be found in both situations. Other examples stem from different kinds of nerve axons. Myelinated nerve axons come with a periodic sequence of myelin cells that insulate the axon except for gaps, the nodes of Ranvier. Hence, these create an (at least partially) discrete medium, while unmyelinated nerve axons form an effectively continuous medium. Moreover, the action potential in myelinated nerves propagates by an overall much faster saltatory conduction, which has a discrete jumping character, while the temporal process in unmyelinated axons is effectively a continuous translation. These differences appear in the aforementioned discrete versus continuous modelling, and one may be more suitable than the other depending on the context. A common feature is that head-on collisions of action potentials (typically) lead to annihilation. We refer to [13,20] for more details and further references.

While the existence of arbitrary local pulse trains and their annihilation is trivial in the GHCA, already the existence proof of a single pulse in FHN is not. It is well known that

FHN possesses a homoclinic travelling wave solution that is spatially asymptotic to a stable rest state and thus corresponds to a single local pulse in GHCA; by spatial reflection the direction of motion can be reversed. However, there is no meaningful notion of a *local* pulse since the spatial coupling by diffusion is effectively non-local through its infinite propagation speed. An analogue of pulse trains on the level of initial data is a superposition of multiple travelling wave pulses placed at a distance from each other. In the dynamics of the PDE, diffusivity immediately couples these pulses, albeit in a weak form. In the past decades, a number of results have been obtained that rigorously relate positions of these ‘pulses’ to an ordinary differential equation system (ODE) [17,54]. However, to our knowledge there are no analytical results for collisions of excitation pulses in higher order equations or systems of PDE—the closest result is the existence of an attracting invariant manifold for a sufficiently distant pair of counter-propagating pulses [48,53]. The situation simplifies for scalar parabolic equations; in particular, the comparison principle for scalar parabolic equations allows to study collisions. We note that also energy methods can be used [51], even for the fourth order (non-excitable) Cahn-Hilliard equation [49].

In this paper we consider suitable scalar parabolic PDE for periodic phase dynamics as models for excitable media, and study similarities and differences between this and the local pulse dynamics of the GHCA. These so-called θ -equations for oscillator phase dynamics [8,41] are given by

$$\theta_t = \theta_{xx} + f(\theta), \quad \theta(t, x) \in S^1 = \mathbb{R}/2\pi\mathbb{Z}, \quad x \in \mathbb{R}, \quad t > 0. \quad (1)$$

For simplicity, we specify the nonlinearity as $f(\theta) := \cos(\theta + \Theta_0) + f_0$, where $f_0 \in (0, 1)$ and $\Theta_0 \in (0, \pi)$ is chosen uniquely so that $f(0) = 0$, although all results are valid in general for the excitable case $|f_0| < 1$ of [41]. More specifically, up to symmetry, the presented analysis is the same for $f_0 \in (-1, 0)$ and the case $f_0 = 0$ is not relevant for our purposes as it supports standing front solutions only.

Equation (1) possesses the stable spatially homogeneous state $\theta \equiv 0$ and a right-moving (as well as left-moving upon reflection) travelling wave solution $\theta(t, x) = \check{\varphi}(\xi)$, $\xi = \pm x - ct$ with speed $c > 0$. The profile $\check{\varphi}(\xi)$ is asymptotic to $0 \in S^1$ for $|\xi| \rightarrow \infty$, but with non-trivial winding number. This means that upon lifting S^1 to \mathbb{R} , the rest state maps to the sequence $2k\pi$, $k \in \mathbb{Z}$, and $\check{\varphi}$ maps to heteroclinic *front* solutions $\varphi + 2\pi k$ with $\varphi(\xi) \rightarrow 0$ as $\xi \rightarrow \infty$, and $\varphi(\xi) \rightarrow 2\pi$ as $\xi \rightarrow -\infty$.

We remark that other wave forms occur in (1), in particular pulses (homoclinic) and wavetrains (periodic), and—near the transition to oscillatory behaviour ($|f| = 1$)—also other coherent structures are possible [8]. However, in the simple GHCA, whose local dynamics has exactly one steady state, these have no counterpart. It might be possible to make relations by introducing subthreshold states in GHCA that create one stable and one unstable state in the local rule.

The choice of f explicitly relates (1) to the overdamped limit of the Sine-Gordon equation, which also arises as a phase field model for certain complex Ginzburg-Landau equations with broken gauge symmetry [2, eqn. (91)]. Following the terminology of the Sine-Gordon equation, we refer to these fronts as *kinks*, and their left-moving spatial reflection as *antikinks*.

In the present context we view these as corresponding to a single local pulse in GHCA. We are thus concerned with the evolution of initial data built from kink- and antikink sequences, such as plotted in Fig. 1. For any given solution $u(x, t)$ viewed in the lift to \mathbb{R} , we geometrically define the set of positions of potential kinks and antikinks through the phase π intercepts as

$$P(u(t)) := \{\xi \in \mathbb{R} \mid \exists k \in \mathbb{Z} : u(\xi, t) = (2k + 1)\pi\}, \quad (2)$$

which readily turns out to be a discrete set for $t > 0$. We will discuss conditions under which this set meaningfully encodes kink or antikink positions also for large $t \gg 1$. A crucial ingredient is the theory of terraces.

Roughly speaking, a terrace is a superposition of finitely many fronts, each of them being a heteroclinic connection between two equilibria, such that asymptotically these fronts are separated, i.e., the distances between any two fronts diverge. To our knowledge, the terminology was introduced in [14], even though the notion was already present in the seminal paper [21] for fronts with distinct speeds. Since then, it appeared that this notion is fundamental in the understanding of the long time behaviour of solutions of reaction-diffusion equations. Poláčik proved in [39] under mild assumptions, in the context of scalar homogeneous semi-linear parabolic equations, that any front-like initial data eventually leads to a terrace profile. These results were extended to localized initial data in [36], leading to a pair of terrace profiles going in opposite directions. Risler independently proved similar results in the more general context of gradient flows in [42] for systems.

When all the considered fronts travel at asymptotically distinct speeds, the behaviour of the terrace profile, the convergence toward it (starting from front-like initial data, for example), as well as its stability are quite well understood, see [33,39] and references therein. On the other hand, if two consecutive fronts have the same asymptotic speed, the question is much more intricate since the eventual separation is powered by weak interactions. In our context, kinks are right moving fronts, while antikinks are left moving fronts, all at the same speed.

Hence, the model (1) is suited for a comparison with GHCA as it allows to study the combination of strong interactions, when a kink and an antikink collide, and weak interactions when considering consecutive kinks. However, this observation already suggests a multi-scale nature, which turns out to imply a fundamental difference for the long time dynamics of excitation pulse positions.

We informally summarize our main results. Suited to unbounded kink-antikink initial data, we prove global well-posedness for unbounded data, and infer that the set of geometric positions (2) consists of isolated points that lie on smooth curves except possibly at collisions. On the one hand, as a qualitative analysis, we rely on the comparison principle and roughly track positions which allows us to show that the minimal initial distance is a global lower bound for distances, and to abstractly identify collision times and locations. Moreover, as a model for the dynamics far from collisions, we show that under periodic boundary conditions the distances of neighboring kinks asymptotically equalise, and we numerically corroborate that this loss of information happens more broadly. On the other hand, as a quantitative analysis, we derive the ODE in the weak interaction regime following [17,43] for finitely many kinks and analyse these in some detail, which extends the aforementioned qualitative terrace results. Our analysis relies on blow-up type singular rescaling and identifies the dynamics as being slaved to dynamics on a sphere at infinity, which, for instance, shows that distances become ordered in finite time. The latter is again hinting a loss of information through the dynamics: the memory of the initial distances is ‘washed out’. This suggests that the chaotic dynamics of GHCA and the entropic complexity based on positional dynamics is reduced by the weak interaction in the PDE, and we do not expect a topological entropy (in a suitable sense for the PDE)—based on positions alone—which resembles that of GHCA.

This paper is organized as follows. In Sect. 2 we discuss the notions of positions and the initial data. Section 3 is devoted to qualitative and quantitative aspects for bounded monotone data which are composed solely of kinks (or antikinks). In Sect. 4, we focus on the annihilation process for initial data composed of kinks and antikinks. Unbounded initial data,

i.e., infinitely many kinks and antikinks, as well as the long-time complexity are considered in Sect. 5. Finally, in Sect. 6 we conclude with a discussion. In the appendices we collect some technical proofs as well as notes on the numerical implementations.

2 Kinks and Anti-kinks and their Positions

In this section we introduce initial data which has imprinted positions of kinks and anti-kinks such that the setwise definition of ‘positions’ $P(u(t))$ in (2), which is well-defined as long as $u(t)$ is defined, turns into meaningful individual positions for all time. In order to discuss this further, we first turn to the notion of kinks and anti-kinks in more detail.

The aforementioned regime $f_0 \in (0, 1)$ is termed excitable since the ODE for spatially constant data possesses a stable rest state and an unstable state which acts as a threshold for undergoing an ‘excitation loop’, i.e., winding once through S^1 . For $f_0 > 1$ the two equilibria have undergone a saddled-node bifurcation and the dynamics of this ODE is a permanent oscillation. We therefore fix an arbitrary $f_0 \in (0, 1)$ throughout.

Travelling waves of (1) with velocity c solve the ODE, considered in \mathbb{R}^2 , given by

$$u_\xi = \phi, \quad \phi_\xi = -c\phi - f(u), \tag{3}$$

and the fundamental *kinks* are fronts, i.e., heteroclinic connections between the stable states $2\pi(k + 1), 2\pi k, k \in \mathbb{N}$. They are strictly monotone decreasing in u and their unique existence (with $f_0 \in (0, 1)$) follows, e.g., by phase plane analysis, cf. [41]. For $k = 0$, we denote the unique translate such that $u(0) = \pi$ by φ and note that $c > 0$; the basic *antikinks* are translates of the spatial reflection $\varphi(-\xi)$. As a scalar reaction-diffusion equation, fronts in (1), and therefore φ as well as $\varphi(-\cdot)$, are orbitally stable [21,46]. We note that due to the periodicity in u , there do not exist heteroclinic orbits connecting $2\pi k$ and $2\pi k'$ for $k - k' \neq 1$.

We use the term kink and antikink more loosely for monotone pieces of $u(\cdot, t)$ that connect even multiples of π . Concerning their positions, we refer to elements in the set P from (2) as *geometric* positions and will introduce a notion of *analytic* positions in Sect. 2.2. These types of positions generally differ, but—as will be shown—the long term dynamics leads to large distances for which the geometric and analytic positions will be exponentially close to each other. In particular, $P(\varphi(t)) = \{ct\}$ is trivially a single point for all time moving with speed c .

As outlined before, we are interested in the relative motion of sequences kinks and antikinks that resemble superpositions of shifted φ and $\varphi(-\cdot)$. We start by considering discontinuous initial data built from kink or antikinks steps,

$$H^-(x) := \begin{cases} 2\pi, & x < 0 \\ \pi, & x = 0 \\ 0 & x > 0 \end{cases}, \quad H^+(x) := \begin{cases} 0, & x < 0 \\ \pi, & x = 0 \\ 2\pi, & x > 0. \end{cases}$$

Notably, the solution with initial data H^- will converge to the above kink φ , while that with initial H^+ converges to the antikink. Next, we consider initial positions

$$\xi_m^- < \xi_{m-1}^- < \dots < \xi_1^- < \xi_1^+ < \xi_2^+ < \dots < \xi_n^+ \tag{4}$$

for m kink and n antikink steps that are shifted to these positions via

$$H_j^\pm(x) := H^\pm(x - \xi_{j+1}^\pm).$$

For convenience, we smoothen H_j^\pm in such a way that the geometric positions $P(u_0)$ of the resulting u_0 coincide with those in (4). This can be realised by replacing H_j^\pm with a convolution $H_{j,\varepsilon_j^\pm}^\pm := \rho_{\varepsilon_j^\pm} * H_j^\pm$ for a positive, symmetric and smooth mollifier ρ_ε supported on $[-\varepsilon, \varepsilon]$ and sufficiently small ε_j^\pm depending on the neighboring initial positions, e.g., $\varepsilon_j^\pm < \frac{1}{2} \min\{|\xi_j^\pm - \xi_{j-1}^\pm|, |\xi_j^\pm - \xi_{j+1}^\pm|\}$ for $2 \leq j \leq n - 1$ and correspondingly for $j = 1, n$. Hence, we set

$$u_0(x; m, n) := \sum_{j=0}^{m-1} H_{j,\varepsilon_j^-}^-(x) + \sum_{j=0}^{n-1} H_{j,\varepsilon_j^+}^+(x). \tag{5}$$

with $n, m \in \overline{\mathbb{N}}_0 := \mathbb{N} \cup \{0, \infty\}$, i.e., possibly infinitely many kink or antikink steps. Due to the separated smoothened intervals the geometric positions of u_0 coincide with (4), i.e., $P(u_0(x; m, n)) = \{\xi_1^-, \dots, \xi_m^-, \xi_1^+, \dots, \xi_n^+\}$.

In the following we omit the dependence on ε_j^\pm since these do not influence the results.

2.1 Well-Posedness

We consider possibly unbounded initial data, which in particular covers the case of infinitely many kinks or antikinks. In order to ensure well-posedness, one option is to consider a weight function $\omega: \mathbb{R} \rightarrow \mathbb{R}$, $\omega(x) := C^{-1}e^{-C|x|}$ for some $C > 0$, and the Banach space

$$X_\omega := \left\{ v(\cdot) \in C(\mathbb{R}) : \omega v \in L^\infty(\mathbb{R}) \right\}, \quad \|v\|_{X_\omega} := \|\omega v\|_\infty := \sup_{x \in \mathbb{R}} |v(x)\omega(x)|.$$

Theorem 1 *For f from (1) the initial value problem*

$$\begin{cases} u_t = u_{xx} + f(u), & u(x, t) \in \mathbb{R}, (x, t) \in \mathbb{R} \times \mathbb{R}_{>0} \\ u(x, 0) = u_0(x) \in X_\omega, & x \in \mathbb{R} \end{cases}$$

has a unique solution $u \in C^\infty(\mathbb{R} \times \mathbb{R}_{>0}, X_\omega)$.

Proof The proof directly follows nowadays classical techniques, and we refer to the milestone monograph [34] for further details. Let us just briefly recall the main steps. Rephrasing the initial value problem as an integral equation, the local existence of a unique solution can be deduced from a standard fixed point argument. To this end, we consider the operator $\Phi: C([0, T], X_\omega) \rightarrow C([0, T], X_\omega)$ defined by

$$\Phi[u] := G_t * u_0(x) + J(x, t), \quad J(x, t) := \int_0^t \int_{\mathbb{R}} G_{t-s}(x - y) f(u(s, y)) dy ds \tag{6}$$

where $u(x, \cdot) \in C([0, T], X_\omega)$ for $x \in \mathbb{R}$ and $G(x, t) := G_t(x) := \frac{1}{\sqrt{4\pi t}} e^{-\frac{|x|^2}{4t}}$, $t > 0$, is the heat kernel. Moreover, by proving the Hölder continuity of this solution, a boot-strap argument shows smoothness of the solution both in x and t .

As for ODE with bounded vector fields, the local existence of the solution can be extended to global existence ($t > 0$) since T is independent of the initial condition. \square

2.2 Geometric and Analytic Positions

Having established global existence, we turn to the specific notions of positions. First we note that the geometrically defined set of positions $P(u(x, t; m, n))$ gives locally smooth

curves of positions as follows. More details for different types of initial data will be given in the subsequent sections.

Proposition 1 *For any $m, n \in \mathbb{N}_0, n + m > 0$, consider the global solution $u(x, t)$ from Theorem 1 with an initial datum $u_0(x; m, n)$ as in (5). Then the following holds. For any $t \geq 0$ the set $P(u(t))$ is discrete and, if $n + m < \infty$, consists of at most $n + m$ elements. There is $t_1 > 0, t_1 = \infty$ if $nm = 0$, such that for $0 \leq t < t_1$ the set $P(u(t))$ consist of differentiable curves $\xi_m^-(t) < \xi_{m-1}^-(t) < \dots < \xi_1^-(t) < \xi_1^+(t) < \xi_2^+(t) < \dots < \xi_n^+(t)$ that coincide with the initial positions (4) at $t = 0$. Moreover, as long as any two such positions are defined, the number of elements in $P(u(t))$ between these cannot increase.*

This Proposition in particular yields, at least locally in time, well-defined and regularly varying positions $\xi_j^\pm(t)$; we refer to $\xi_j^-(t)$ as kink positions and $\xi_j^+(t)$ as antikink positions.

Proof This proposition is a consequence of the properties of the number of zeros for linear parabolic equations, see [4,45] for a rigorous exposition and we refer to [40, §2.3] for an exposition of the results used next.

Let $v = \partial_x u$ be the spatial derivative of the solution. Given u , it solves a linear parabolic equation, and at $t = 0$ the minimum of u yields a sign change of v at a locally unique zero. The intervals where u is constant occur on monotone parts of u and are thus not associated to non-trivial sign changes of v .

It follows from the zero number principle that there exists $T \in (0, \infty]$ such that v has a unique simple zero on $(0, T)$, and has constant sign on (T, ∞) . Moreover, from parabolic regularity and the implicit function theorem, there exists a C^1 function $t \mapsto \eta(t)$ such that $v(\eta(t), t) = 0$, for all $t \in (0, T)$. This implies that the set $P(u(t))$ is discrete for all $t \geq 0$ and, again from the implicit function theorem, that each point lies on a differentiable curve.

Let us now turn to the case $n + m < \infty$. Let β_0^\pm be the value of u_0 at $x \rightarrow \pm\infty$. Then (see [50, Theorem 4.4.2], for instance)

$$\beta^\pm(t) := \lim_{x \rightarrow \pm\infty} u(x, t).$$

exists for all $t \geq 0$, and are solutions of the initial value problem

$$\dot{\beta}^\pm = f(\beta^\pm), \quad \beta^\pm(0) = \beta_0^\pm$$

in particular, due to our choice of initial condition (5), it follows that these limits are constant steady states of the above equation. Combined with the sign properties of $\partial_x u$, this proves that $P(t)$ consists of at most $n + m$ elements.

It remains to prove that the cardinality of $P(t)$ is non-increasing. We claim that if there exists k_0, t_0 such that $u(\eta(t_0), t_0) = (2k_0 - 1)\pi$, then $u(\cdot, t) > (2k_0 - 1)\pi$ for all $t > t_0$. This is a consequence of the maximum principle: let $\alpha(t)$ be a solution of the initial value problem

$$\dot{\alpha} = f(\alpha), \quad \alpha(t_0) = (2k_0 - 1)\pi.$$

Then $t \mapsto \alpha(t)$ is increasing and converges to $2k_0\pi$ as $t \rightarrow \infty$. Let $w(x, t) = u(x, t) - \alpha(t)$. Then, taking u as given, w solves a linear parabolic equation on (t_0, ∞) , and $w(\cdot, t_0) \geq 0$. It follows that $w(\cdot, t) > 0$ for all $t > t_0$, which concludes the claim and the proof. \square

In particular, for the solution $u_*(x, t)$ with a single smoothed jump kink initial data $u_*(x, 0) = H_\varepsilon$, there is a unique globally defined geometric position $P(u(t)) = \{\xi_*(t)\}$. We denote its speed as $c_* := \frac{d}{dt}\xi_*$. Recall that the single kink speed is denoted by c , and the aforementioned convergence result of u_* to the kink φ implies $c_*(t) \rightarrow c$ as $t \rightarrow \infty$.

In order to study the evolution of distances between kinks or antikinks in more detail, it is convenient to define the following analytic positions, which however requires sufficiently large initial distances $\xi_i - \xi_{i+1}$ ($1 \leq j \leq n$) between neighboring kinks.

The broader task of deriving laws of motion for localized states in terms of ordinary differential equations (“laws of motion”) dates back at least to the studies on metastable fronts in the Allen-Cahn equation by Carr-Pego and Fusco-Hale, who derived ODEs for the analytic positions of fronts, cf. [10,18,21]. This has been explored in various directions, notably to infinitely many metastable pulses in arbitrary dimension [54]; we mainly follow [17] and [43].

This allows to derive such ODE rigorously only for sequences of either kinks or antikinks, i.e., monotone initial data, and we therefore restrict attention to (5) with $m = 0$. Since in this case the overall motion of kink initial data is dominated by the drift with velocity c , we consider the deviation from this speed by introducing the comoving frame $z = x - ct$, which introduces the term $c\partial_z u$ on the right hand side of (1) and yields, in the covering space \mathbb{R} ,

$$u_t = u_{zz} + cu_z + f(u). \tag{7}$$

The corresponding solution $u(z, t)$ is defined globally in $t \geq 0$ by Theorem 1. We will define analytic positions $\eta_i(t)$ that relate to the geometric positions ξ_i by $ct + \eta_i(t) \approx \xi_i(t)$.

For sufficiently large initial distances, the analytic positions are defined by writing $u(z, t)$ as

$$u(z, t) = \sum_{i=1}^n \varphi_i(z, t) + w(z, t), \quad \varphi_i(z, t) := \varphi(z - \eta_i(t)), \tag{8}$$

with η_i ($1 \leq j \leq n$) uniquely defined through the following orthogonality condition on w as detailed in “Appendix A”. Let $L_i := \partial_z^2 + c\partial_z + f'(\varphi_i)$ denote the linearized operator of the right hand side of (7) in φ_i , and $L_i^* := \partial_z^2 - c\partial_z + f'(\varphi_i)$ its adjoint. The remainder term w is now supposed to be orthogonal to the adjoint eigenfunctions $e_i^* := e^{c(z-\eta_i)}\varphi_i'$, i.e.

$$\langle w, e_i^* \rangle = \int_{\mathbb{R}} e^{c(z-\eta_i)} w(z, t) \varphi_i'(z, t) dz = 0, \quad 1 \leq i \leq n. \tag{9}$$

For initial data as in (5), w is initially nonzero, so that for the study of analytic positions it is natural—though not necessary—to replace $H_{k,\varepsilon}^\pm$ by the fronts, i.e., φ_i as in (8). Then $w(z, 0) \equiv 0$ and thus remains small at least for short time. In order to control w also for larger times, we assume that the kinks are initially well-separated, i.e., $|\eta_i(0) - \eta_{i-1}(0)| \gg 1$ ($2 \leq i \leq n$).

Remark 1 For initial data v_0 as in (8), the set $P(v_0)$ does not coincide with the initial positions (4), though the error is exponentially small in the minimal distance. Moreover, for $nm > 0$, the set $P(v_0(\cdot; m, n))$ may contain spurious points such that one generally needs to assume a minimal distance between ξ_1^- and ξ_1^+ .

Remark 2 For any fixed t and i , the analytic kink position $\eta_i(t)$ equals the (shifted) geometric position $\xi_i(t) - ct$ if and only if $w(\xi_i(t), t) = (n - 1)\pi - \sum_{j=1, j \neq i}^n \varphi(\xi_j(t) - ct - \eta_j(t))$, as can be seen from (8). In particular, all geometric and analytic positions coincide if and only if w vanishes simultaneously at all geometric positions. However, kinks interact eventually repulsively, i.e., their distances eventually increase (see Sect. 3 below for details) and this implies $\|w(\cdot, t)\| \rightarrow 0$ as $t \rightarrow \infty$ (in L^2 or L^∞) so that both definitions asymptotically coincide.

3 Bounded Monotone Initial Kink Data

In this section we consider bounded monotone data which are composed of kinks and analyse the distances between neighboring kinks in terms of the geometric as well as analytic positions. We note that by spatial reflection the discussion equally applies to bounded sequences of antikinks. First we track geometric positions via the comparison principle, which applies for any initial distance, but only constrains the positions to lie within certain intervals, referred to as *gaps*, that also depend on the initial data. The analytic positions provide more specific laws of motion that apply immediately for initial data with sufficiently distant positions, or—more abstractly—from some point in time onward with a distribution of positions for which we just know the positions up to the gaps.

The latter relies on the results by Poláčik and Risler, which state that front-like initial data converge to a terrace whose speeds converge and whose distances *eventually* diverge, albeit without a quantitative estimate. For our purposes, this can be summarized as follows.

Theorem 2 *cf. [39,42] Let $-\pi < u_0 < 2\pi(k + 1)$ ($k \in \mathbb{N}$) be an initial datum with $\lim_{x \rightarrow -\infty} u_0(x) = 2\pi k$, $\lim_{x \rightarrow \infty} u_0(x) = 0$ and corresponding solution u . Then there exist C^1 functions ξ_1, \dots, ξ_k on \mathbb{R} satisfying*

$$\lim_{t \rightarrow \infty} \xi'_j(t) = 0 \quad (j = 1, 2, \dots, k), \quad |\xi_j(t) - \xi_{j+1}(t)| \rightarrow \infty \quad (j = 1, 2, \dots, k - 1)$$

such that the solution $u(\cdot, t)$ converges to the corresponding terrace:

$$\left\| u(\cdot, t) - \sum_{j=1}^k \varphi(\cdot - ct - \xi_j(t)) \right\|_{\infty} \xrightarrow{t \rightarrow \infty} 0$$

Remark 3 In Proposition 3 below we give a lower bound on the distances which is of course far from optimal in the asymptotics $t \rightarrow \infty$. Naively, one might suppose that all distances monotonically increase; however, this is not true in general, as the results in Sect. 3.2 show, and numerical simulations illustrate, cf. Fig. 4a, b.

In order to describe the long-time behaviour of bounded solutions under kink-antikink annihilations, we consider limit sets. For bounded monotone solutions, this has already been done—for a much broader setup—in [39] from which we take the following definition of the limit set

$$\Omega(u) := \{v : u(\cdot + x_n, t_n) \rightarrow v \text{ for some sequences } t_n \rightarrow \infty \text{ and } x_n \in \mathbb{R}\},$$

where $u \in L^\infty(\mathbb{R} \times \mathbb{R}^+)$ and the convergence is in $L^\infty_{loc}(\mathbb{R})$ (locally uniform convergence). Compared to the standard definition of ω -limit set, this allows to observe any finite piece of the graph of $u(\cdot, t_n)$. For the special situation of Theorem 2, the set is given by

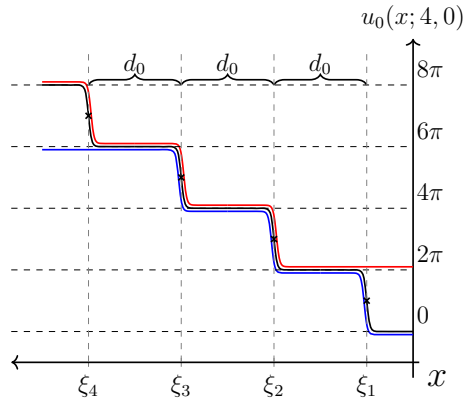
$$\Omega(u) = \{\varphi(\cdot - \tau) : \tau \in \mathbb{R}\} \cup \{2\pi j : j = 0, 1, \dots, k\}, \tag{10}$$

cf. [39]. Our results add the description of ω and Ω in case $m + n < \infty$ and $mn \neq 0$, even though they are consequences of (10) after pairwise annihilations of kinks and antikinks.

3.1 Qualitative Aspects: Comparison Principle

Let $u_0(x; n) := u_0(x; n, 0)$ be a monotone initial datum (5) without antikinks and associated global solution $u(x, t; n)$; recall the positions are globally defined and differentiable

Fig. 2 Sketch of initial datum $u_0(x; 4)$ (black) with four antikinks at equidistant positions $\xi_i(0), i = 1, 2, 3, 4$, such that $u(\xi_i(0), 0) = (2j + 1)\pi$. The blue initial datum is given by u_0 with position $\tau_j(0) = \xi_j(0)$ for $j = 1, 2, 3$ while the red one is given by \bar{u}_0 with positions $\psi_j(0) = \xi_{j+1}(0)$ for $j = 1, 2, 3$. For the purpose of illustration, the curves are plotted slightly below and above $u_0(x; 4)$, respectively



according to Proposition 1. Since the data has kinks only we omit the superindex ‘-’ and also introduce the following notation for the speeds of positions, the nearest distances and the minimal distance (starting from a given position):

$$c_i(t) := \frac{d}{dt} \xi_i(t), \quad 1 \leq i \leq n, \tag{11}$$

$$d_j(t) := \xi_j(t) - \xi_{j+1}(t), \quad 1 \leq j \leq n - 1 \tag{12}$$

$$\underline{d}_i(t) := \min_{i \leq j \leq n-1} d_j(t), \tag{13}$$

as well as $d_{\min}(t) := \underline{d}_1(t)$.

Equidistant kinks. Let us first consider initial data composed of equidistant antikinks, cf. Fig. 2, as it is straightforward to construct sub- and supersolutions in order to compare the speeds (11) and, consequently, to find a uniform lower bound on the distances (12).

Proposition 2 *Let $u(x, t; n)$ ($n \geq 2$) be the solution with an initial datum $u_0(x; n)$, where $d_i(0) = d_0$ for all $1 \leq i \leq n - 1$ for some constant $d_0 > 0$. Then $c_1(t) \geq c_*(t) \geq c_n(t)$ for all $t \geq 0$, and $c_1(0) \geq c_2(0) \geq \dots \geq c_n(0)$. In particular, initially all distances $d_i(0)$ are non-decreasing in t and $d_i(t) \geq d_0$ for all $t > 0$.*

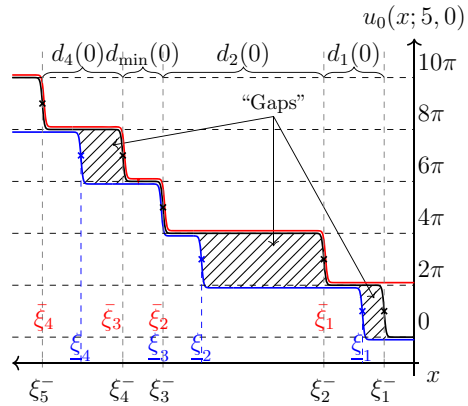
Proof We will consider solutions $u(x, t; k)$ for initial $u_0(x; k)$ with positions $\xi_j, j = 1, \dots, k$ with $k < n$. That is, the positions of $u_0(x; k)$ build a proper subset of $\{\xi_i : 1 \leq i \leq n\}$ which contains the positions of $u_0(x; n)$. We compare the speeds of kinks which we therefore denote as c_j^k , where we omit the argument t for readability; hence, $c_* = c_1^1$. Recall that by c_* , we denote the speed of the solution $u_*(x, t)$ with a single smoothed jump kink initial datum H , cf. Sect. 2.2.

We first prove the statement for $n = 2$. In this case, the initial datum $u_0(x; n)$ is sandwiched by $H(x - \xi_1) \leq u_0(x; n) \leq H(x - \xi_2) + 2\pi$ for all $x \in \mathbb{R}$. By the comparison principle, for the solution $u_*(x, t)$ with $u_*(x, 0) = H(x)$, we have $u_*(x - \xi_1 + 1, t) \leq u(x, t; n) \leq u_*(x - \xi_2, t) + 2\pi$ for all $(x, t) \in \mathbb{R} \times \mathbb{R}_+$. Since both H_0 and H_1 move with the same speed c_* , the speeds of the kinks satisfy $c_1^2 \geq c_* \geq c_2^2$ for all $t \geq 0$.

For $n \geq 3$, we choose sub- and supersolutions composed of $n - 1$ antikinks (cf. Fig. 2). More precisely, let $u_0(x; n - 1)$ be the initial condition composed of $n - 1$ kinks with the same $n - 1$ positions, $\xi_i(0)$ for $2 \leq i \leq n$, as $u_0(x; n)$. The comparison solutions arise from the initial data

$$\underline{u}_0(x) := u_0(x - d_0; n - 1), \quad \bar{u}_0(x) := u_0(x; n - 1) + 2\pi.$$

Fig. 3 Sketch of gaps (hatched): $\xi_{\bar{i}}(0) < \xi_i(0)$ for $i = 1, 2, 4$. The associated speeds need not be ordered. In particular, the distances may be increasing or decreasing



In particular, the kink positions of \underline{u}_0 are $\xi_i(0)$ for $1 \leq i \leq n - 1$ and those of \bar{u}_0 are $\xi_i(0)$ for $2 \leq i \leq n$.

Since \underline{u} and \bar{u} are translates of each other, their positions $\xi_{\bar{i}}, \bar{\xi}_i, 1 \leq i \leq n - 1$ are equal up to shift by d_0 and have the same speeds c_i^{n-1} , for all $t \geq 0$. By construction, $\underline{u}_0 \leq u_0 \leq \bar{u}_0$ and thus the corresponding solutions satisfy $\underline{u} \leq u(\cdot; n) \leq \bar{u}$ for all $(x, t) \in \mathbb{R} \times \mathbb{R}_+$ by the comparison principle. We can therefore compare the speeds c_j^n with the speeds c_i^{n-1} of positions in \underline{u} and \bar{u} , respectively, which leads to the following relations for all $t \geq 0$:

$$c_1^n \geq c_1^{n-1}, \quad c_j^{n-1} \leq c_j^n \leq c_{j-1}^{n-1} \text{ for } 1 < j < n, \quad c_n^n \leq c_{n-1}^{n-1}.$$

Hence, $c_i^n \geq c_i^{n-1} \geq c_{i+1}^n$ for $i = 1, \dots, n - 1$. By iterating this construction of sub- and supersolutions, $c_1^n \geq c_1^{n-1} \geq \dots \geq c_1^2 \geq c$ and, analogously, $c_n^n \leq c_{n-1}^{n-1} \leq \dots \leq c_2^2 \leq c$ for all $t \geq 0$. \square

We note that the proof of Proposition 2 shows that there is a hierarchy of speeds when removing kinks on the left or right. Up to equality in the bounds, kinks for equidistant data spread out, and the more kinks there are, the faster the spreading can be.

Non-equidistant kinks. For more general initial data, only the overall distance $\xi_n(t) - \xi_1(t)$ and the smallest distance $d_{\min}(t)$ can be controlled by our approach of sub- and supersolutions: lower bounds can be inferred for the distances only up to “gaps” rooted in the initial data. In these gaps the ordering of the associated positions and speeds cannot be further constrained by this method, cf. Fig. 3. In view of the upcoming analysis based on analytic positions, this is not surprising since distances may behave non-monotonically.

Proposition 3 *The solution to any initial $u_0(x; n), n \geq 2$, satisfies the following for all $t \geq 0$:*

$$\begin{aligned} \frac{d}{dt}(\xi_n(t) - \xi_1(t)) &\geq 0, \quad c_1(t) \geq c_*(t) \geq c_n(t), \\ d_i(t) &\geq d_{\min}(0) \quad \forall t > 0, \quad 1 \leq i \leq n - 1. \end{aligned} \tag{14}$$

Moreover, if $d_{\min}(0) = d_j(0)$ for some $1 \leq j \leq n - 1$ and $t \geq 0$ then $d_j(t)$ is non-decreasing for all $t \geq 0$. In particular, $d_{\min}(t)$ is non-decreasing at least as long as the minimal distance is realised at the same index as initially.

Proof The proof is analogous to that of Proposition 2. Comparing u with single kinks shifted to ξ_1 as a subsolution and to ξ_n as a supersolution we immediately infer $c_1(t) \geq c_*(t) \geq c_n(t)$

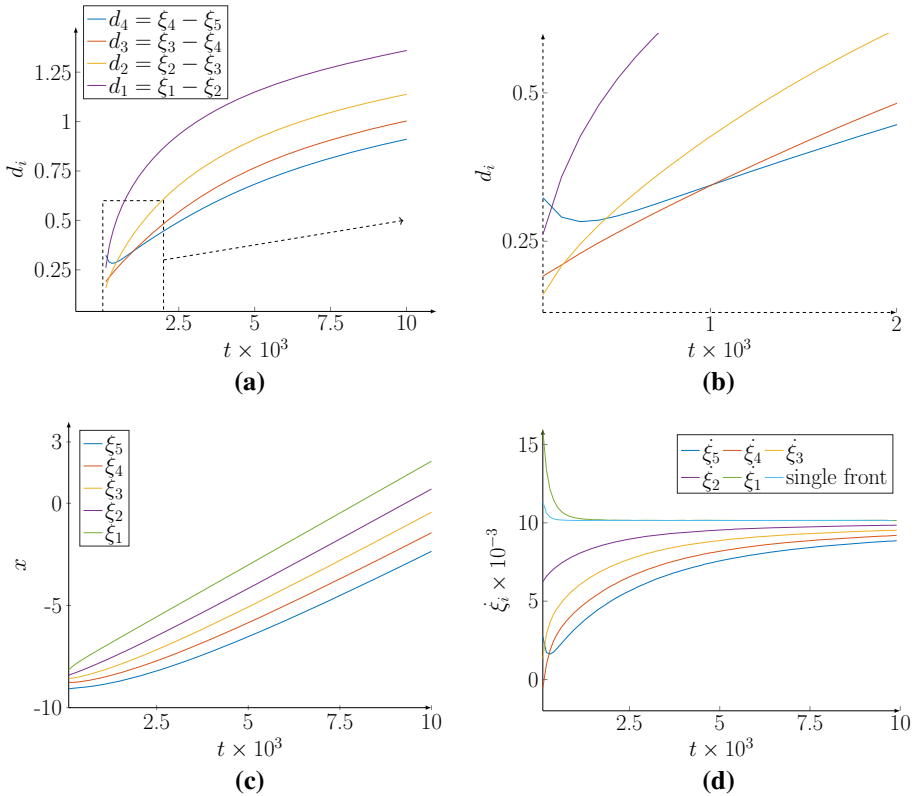


Fig. 4 Simulation of kink distances (a) (with zoom (b)), positions (c) and speeds (d), starting from an initial condition with five kinks and $f_0 = 0.2$. As can be seen from (a) and (b), the distances need not be monotone functions, but are eventually ordered, cf. Sect. 3.2. Moreover, the speeds of the kinks converge to the single front speed (d)

so that $\frac{d}{dt} (\xi_n(t) - \xi_1(t)) \geq 0$. Next, we replace d_0 in the proof of Proposition 2 by $d_{\min}(0)$ and use again $\bar{u}_0(x) := u_0(x - d_{\min}(0); n - 1)$, as well as $\underline{u}_0 := u_0(x; n - 1) + 2\pi$, cf. Fig. 3. By the comparison principle this implies for all $t \geq 0$ the relations $c_i^n \leq c_{i-1}^{n-1}$ for $2 \leq i \leq n$ from the supersolution, but the subsolution only yields for j such that $d_{\min}(0) = d_j(0)$ the relation $c_j^{n-1} \leq c_j^n$. Taken together we obtain, for all $t \geq 0$,

$$c_j^n \geq c_j^{n-1} \geq c_{j+1}^n,$$

and therefore $\frac{d}{dt} d_j(t) \geq 0$. In particular, $\frac{d}{dt} d_{\min}(t) \geq 0$ as long as the minimal distance is between $\xi_j(t)$ and $\xi_{j+1}(t)$, but at least for $t = 0$. □

As this use of sub- and supersolutions is limited by the described gaps, a substantial part of the next section is devoted to a deeper analysis of the behaviour of the distances in terms of the analytic positions.

3.2 Quantitative Aspects: Projection Scheme

The above discussion, and in particular Proposition 3, gives a first qualitative overview of interactions between stacked fronts traveling at the same asymptotic speed c . The purpose of this section is to obtain deeper insight into the relative laws of motion of the front positions, which is however valid for sufficiently large distances only. As mentioned in Sect. 2.2, we follow an approach that has developed out of the analysis of meta-stability of fronts in Allen-Cahn equation in [10,18].

Recall the notion of analytic positions from (8), (9), and denote $\eta := (\eta_1, \dots, \eta_n)$ as well as

$$\delta_j := \eta_j - \eta_{j+1}, \quad \delta_{\min} = \min\{\delta_j, 1 \leq j \leq n - 1\}.$$

Initial data (8) with $w \equiv 0$ form the nested n -dimensional manifolds (with $\delta = \delta_{\min}$)

$$\mathcal{K}_\delta := \left\{ \sum_{j=0}^n \varphi(\cdot + z_0 - \eta_j) : \eta_1 > \eta_2 > \dots > \eta_n, \eta_i - \eta_{i+1} > \delta, i = 1, \dots, n; z_0 \in \mathbb{R} \right\}.$$

Theorem 2 shows that kinks interact eventually repulsively, which can be understood as asymptotic stability of \mathcal{K}_δ for any $\delta > 0$. In this section we will show that, for any sufficiently large δ , \mathcal{K}_δ parametrises an n -dimensional invariant manifold \mathcal{M} , and we study the reduced dynamics on it. Moreover, \mathcal{M} is globally attracting for initial data as in Theorem 2. In particular, any initial datum with initial data from geometric positions (5) is contained in its basin of attraction, if the initial geometric distances are sufficiently large (Fig. 4).

This analysis relies on the following results, which can be inferred from [17]. Although the latter is not intended to specifically study stacked fronts as in his paper, but rather pulses, our situation can be dealt with by exactly the same methods.

We reformulate the results that we use in our notation and towards our purposes, and refer in particular to Theorems 2.1, 2.3 and 4.1 in [17] for proofs. We also provide in ‘‘Appendix A’’ some more details and a derivation of the reduced ODE system, in order to close the gap to [17].

The basic observation is the following well known decomposition in such neighborhoods, which readily follows from an implicit function theorem, cf. ‘‘Appendix A’’. Here we consider neighbourhoods of \mathcal{K}_δ defined as $\mathcal{U}_{\varepsilon,\delta} := \mathcal{K}_\delta + \{v \in H^2(\mathbb{R}) : \|v\|_{H^1} < \varepsilon\}$.

Lemma 1 *There exist $\delta^*, \varepsilon^* > 0$ such that for any $v \in \mathcal{U}_{\varepsilon^*,\delta^*}$, there exist unique $\eta_1, \dots, \eta_n \in \mathbb{R}^n$ and a unique function $w(z) \in H^2(\mathbb{R})$ satisfying*

$$v(z) = \sum_{j=0}^n \varphi(z - \eta_j) + w(z), \quad \int_{\mathbb{R}} e^{cz} w(z) \varphi(z - \eta_j) dz = 0, \text{ for all } 1 \leq j \leq n. \quad (15)$$

We note the following direct consequence of Lemma 1 together with well-posedness.

Proposition 4 *For any solution $u(z, t)$ of (7) whose initial data lies in $\mathcal{U}_{\varepsilon^*,\delta^*}$ we have $T_* := \sup\{t : u(z, s) \in \mathcal{U}_{\varepsilon^*,\delta^*}, 0 \leq s \leq t\} > 0$ and there exist unique functions $\eta_1(t), \dots, \eta_n(t) \in C^1(0, T_*)$, and $w(z, t) \in C^1((0, T_*) \times \mathbb{R})$ such that (8) and (9) hold for all $t \in (0, T_*)$.*

In particular, initial conditions $u_0(x; 0, n)$ from (5) with d_{\min} sufficiently large lie in $\mathcal{U}_{\varepsilon^*,\delta^*}$ so that Proposition 4 applies for those as well.

Building on the decomposition (8), the following proposition, which is a combination of results from [17], cf. ‘‘Appendix A’’, gives a quantitative description of the relative motions

as a reduced ODE for the analytic positions η_j . Relevant for the laws of motion are in particular the eigenvalues of the linearization of (3) in the asymptotic states $(\varphi, \varphi') = (0, 0)$ and $(\varphi, \varphi') = (2\pi, 0)$, which we readily determine as

$$\lambda := \frac{-c - \sqrt{c^2 - 4f'(0)}}{2} < 0, \quad \mu := \frac{-c + \sqrt{c^2 - 4f'(0)}}{2} > 0; \tag{16}$$

recall $f'(2\pi) = f'(0)$ by periodicity of f , and note $\lambda = -\mu - c$.

Proposition 5 *There exist $\delta_* \geq \delta^*, \varepsilon_* \leq \varepsilon^*$ such that $\mathcal{U}_{\varepsilon_*, \delta_*}$ contains an n -dimensional exponentially attractive locally invariant manifold \mathcal{M} , which is a graph over \mathcal{K}_{δ_*} in terms of corrections $w = w(\eta)$ satisfying (15). The reduced n -dimensional dynamics of (7) on \mathcal{M} is given by the following ordinary differential equation system, which is defined for $\delta_{\min} \geq \delta_*$ and where $\alpha, a_R, a_L > 0$, and $\mathcal{R}_j(\eta), 1 \leq j \leq n$, are C^1 -functions; furthermore $\mu + \alpha > -\lambda$ for $f_0 \approx 0$.*

$$\begin{cases} \eta'_1(t) = a_L e^{\lambda(\eta_1 - \eta_2)} + \mathcal{R}_1(\eta) \\ \eta'_j(t) = a_L e^{\lambda(\eta_j - \eta_{j+1})} - a_R e^{-\mu(\eta_{j-1} - \eta_j)} + \mathcal{R}_j(\eta), \quad 2 \leq j \leq n - 1, \\ \eta'_n(t) = -a_R e^{-\mu(\eta_{n-1} - \eta_n)} + \mathcal{R}_n(\eta). \end{cases} \tag{17}$$

The remainder terms $\mathcal{R}_j(\eta)$ and the correction term $w(\eta)$ satisfy, for some constant $C > 0$,

$$|\mathcal{R}_j|, \|w(\eta)\|_{H^2(\mathbb{R})} \leq C e^{-(\mu + \alpha)\delta_{\min}}. \tag{18}$$

Remark 4 Remark that we do not claim that $\mu + \alpha \geq \lambda$ for all $f_0 \in (0, 1)$, which means that the remainder terms \mathcal{R}_j and w are not necessarily higher order compared with the a_L -terms whose exponential rate is λ .

In the remainder of this section we analyse (17) in more detail and in particular infer that, if the initial distance are large enough, then the validity constraint $\delta_{\min} \geq \delta_*$ is satisfied for all $t \geq 0$. This is of course consistent with Theorem 2, which moreover implies that all solutions with certain initial data eventually satisfy (8), (9) and obey (17).

Theorem 3 *There is $\delta_1 \geq \delta_*$ such that $\mathcal{U}_{\varepsilon_*, \delta_1}$ is forward invariant for (7). In particular, the decomposition (8), (9) and the ODE (17) are valid for all $t \geq 0$. Moreover, for any solution $u(z, t)$ with initial datum as in Theorem 2, there is $t_1 \geq 0$ such that $u(\cdot, t_1) \in \mathcal{U}_{\varepsilon_*, \delta_1}$.*

Proof The proof is given in Sect. 3.2.4. □

The analysis of (17) is facilitated by normalizing $\tilde{\delta}_i := \mu \delta_i(t/\mu)$ and setting $\tilde{\delta}_{\min} := \min\{\tilde{\delta}_1, \dots, \tilde{\delta}_n\}$, $\varepsilon := \min\{\alpha, c\}/\mu$, so that (17) takes the form

$$\begin{aligned} \tilde{\delta}'_1 &= e^{-\tilde{\delta}_1} + g_1 e^{-(1+\varepsilon)\tilde{\delta}_{\min}}, \\ \tilde{\delta}'_j &= e^{-\tilde{\delta}_j} - e^{-\tilde{\delta}_{j-1}} + g_j e^{-(1+\varepsilon)\tilde{\delta}_{\min}}, \end{aligned} \tag{19}$$

where $g_j, 1 \leq j \leq n$, are bounded. Note that while $\tilde{\delta}_{\min}$ is in general only Lipschitz continuous due to the minimum function, the products $g_j e^{-(1+\varepsilon)\tilde{\delta}_{\min}}, j = 1, 2$ are smooth. For convenience, we extend their domain beyond the definition limit $\tilde{\delta}_{\min} \geq \delta_*$ to smooth functions on \mathbb{R}^n_+ with g_j bounded.

Our aim is to analyze the temporal ordering and asymptotics of the distances $\tilde{\delta}_j, j = 1, 2, \dots, n$. To this end, we consider system (19) as a perturbation of the system with $g_j \equiv 0$ for all $1 \leq j \leq n$, which we refer to as the *unperturbed* system.

3.2.1 The Unperturbed Distance System

For the unperturbed system, i.e. the system,

$$\begin{aligned} \tilde{\delta}'_1 &= e^{-\tilde{\delta}_1}, \\ \tilde{\delta}'_j &= e^{-\tilde{\delta}_j} - e^{-\tilde{\delta}_{j-1}}, \quad 2 \leq j \leq n, \end{aligned} \tag{20}$$

we directly get $\tilde{\delta}'_1 > 0$, that is the rightmost distances is increasing. Moreover, the distance $\tilde{\delta}_j$ ($2 \leq j \leq n$) increases if (and only if) $\tilde{\delta}_j < \tilde{\delta}_{j-1}$, i.e., if the distance between the j -th kink and its left neighbor kink is smaller than the distance to its right neighbor. In particular, the smallest distance at time $t \geq 0$ increases. This motivates the question whether the distances are eventually ordered and which asymptotics are implied by this ordering.

Theorem 4 *There exists $T > 0$ such that $\tilde{\delta}_n(t) < \tilde{\delta}_{n-1}(t) < \dots < \tilde{\delta}_1(t)$ for all $t \geq T$. Moreover, $\lim_{t \rightarrow \infty} \tilde{\delta}_k(t) = \infty$ for all $1 \leq k \leq n$.*

Proof Let us first prove the divergence of the distances by induction over n . The statement is clear for $k = 1$ since $\tilde{\delta}_1(t) = \log(t + C)$, $C > 0$. Suppose the statement holds for δ_k with $2 \leq k \leq n$ and, by contradiction, $\tilde{\delta}_{n+1} \leq M$ for some $M > 0$. Then $\tilde{\delta}'_{n+1}(t) \geq e^{-M} - e^{-\tilde{\delta}_n(t)} > 0$ for t large enough. Consequently, $\tilde{\delta}_{n+1}$ converges, hence $\lim_{t \rightarrow \infty} \tilde{\delta}'_{n+1}(t) = 0$ and thus $\tilde{\delta}_n(t) \rightarrow M$ as $t \rightarrow \infty$, contradicting the induction hypothesis.

As to the eventual ordering, we first show the existence of some $T_1 > 0$ such that $\tilde{\delta}_2(t) < \tilde{\delta}_1(t)$ for all $t > T_1$. To this end, assume by contradiction that for all $t > 0$ there exists some $t_1 > t$ with $\tilde{\delta}_2(t_1) \geq \tilde{\delta}_1(t_1)$, i.e. $\tilde{\delta}'_2(t_1) \leq 0$. By the divergence of the distances, there exists $t_2 > t_1$ with $\tilde{\delta}'_2(t_2) > 0$. Since $\tilde{\delta}_1$ increases monotonically, this implies that $\tilde{\delta}_2$ intersects the $\tilde{\delta}_2$ -nullcline $\{(\tilde{\delta}_1, \tilde{\delta}_2) : \tilde{\delta}_1 = \tilde{\delta}_2\}$ infinitely often. However, this is impossible since the set $\{(\tilde{\delta}_2, \tilde{\delta}_1) : \tilde{\delta}_2 < \tilde{\delta}_1\} = \{(\tilde{\delta}_2, \tilde{\delta}_1) : \tilde{\delta}'_2 > 0\}$ is forward invariant. In particular, if $\tilde{\delta}_2(t) = \tilde{\delta}_1(t)$ for some $t \geq 0$, then $\tilde{\delta}_2(t') < \tilde{\delta}_1(t')$ for all $t' > t$. Analogously, there exists $T_2 > T_1$ with $\tilde{\delta}_3(t) < \tilde{\delta}_2(t)$ for all $t > T_2$. Likewise, for all remaining pairs of distances, there exists some suitable time $T_i > T_{i-1}$. Setting $T := T_1$ concludes the proof. \square

In order to get a result similar to Theorem 4 for the perturbed system, we first reformulate the problem by applying a polar blow-up transformation; this enables us to apply a perturbation argument.

3.2.2 Polar Blow-Up

Substituting $z_j = e^{-\tilde{\delta}_j}$ into (19), and setting $z_{\max} := e^{-\tilde{\delta}_{\min}}$ we obtain the system

$$\begin{aligned} z'_1 &= -z_1^2 - g_1 z_1 z_{\max}^{1+\varepsilon}, \\ z'_j &= -z_j^2 + z_{j-1} z_j - g_j z_j z_{\max}^{1+\varepsilon}, \quad 2 \leq j \leq n \end{aligned}$$

which possesses the non-hyperbolic equilibrium $\mathbf{0} = (0, 0, \dots, 0)^T \in \mathbb{R}^n$. The polar blow-up transformation $z = (z_1, z_2, \dots, z_n)^T = r(t)\Psi(t)$ with $r \in \mathbb{R}$ and $\Psi = (\Psi_1, \Psi_2, \dots, \Psi_n)^T \in S^{n-1}$ yields

$$\begin{aligned} z'_1 &= -r^2 \Psi_1^2 - r^{2+\varepsilon} g_1 \Psi_1 \Psi_{\max}^{1+\varepsilon}, \\ z'_j &= -r^2 \Psi_j (\Psi_j - \Psi_{j-1}) - r^{2+\varepsilon} g_j \Psi_j \Psi_{\max}^{1+\varepsilon}, \quad 2 \leq j \leq n, \end{aligned} \tag{21}$$

where $z_{\max} = r\Psi_{\max}$, i.e., for each t there is j such that $\Psi_{\max}(t) = \Psi_j(t)$. Note that the equilibrium $\mathbf{0}$ corresponds to $r = 0$. The inner product with Ψ gives

$$(z', \Psi) = r'(t) = \sum_{k=1}^n z'_k \Psi_k = -r^2 \Sigma_n - \mathcal{O}(r^{2+\varepsilon}) \tag{22}$$

where $\Sigma_n := \Psi_1^3 - \sum_{k=2}^n \Psi_k^2 (\Psi_{k-1} - \Psi_k)$. Using $z'_k = r' \Psi_k + r \Psi'_k$ together with (22) in (21) we may divide left and right hand sides by r to obtain

$$\begin{aligned} \Psi'_1 &= r\Psi_1(\Sigma_n - \Psi_1) + \mathcal{O}(r^{1+\varepsilon}), \\ \Psi'_j &= r\Psi_j(\Psi_{j-1} - \Psi_j + \Sigma_n) + \mathcal{O}(r^{1+\varepsilon}). \end{aligned}$$

Dividing the right hand side by r results in the desingularised radial and angular equations

$$r' = -\Sigma_n r - \mathcal{O}(r^{1+\varepsilon}), \tag{23}$$

$$\Psi'_1 = \Psi_1(\Sigma_n - \Psi_1) + \mathcal{O}(r^\varepsilon), \tag{24}$$

$$\Psi'_j = \Psi_j(\Psi_{j-1} - \Psi_j + \Sigma_n) + \mathcal{O}(r^\varepsilon), \tag{25}$$

which, for $r > 0$, has the same trajectories as (22) and solutions are related by time rescaling.

Analogous to (20), we consider system (23)–(25) as a perturbation of the unperturbed polar system with g_j set to zero ($1 \leq j \leq n$), i.e., zero error terms in (23)–(25), which means

$$r' = -\Sigma_n r, \tag{26}$$

$$\Psi'_j = \Psi_j(\Sigma_n - \Psi_j + \Psi_{j-1}), \quad 1 \leq j \leq n, \quad \Psi_0 := 0. \tag{27}$$

We remark that directions to infinity for $(\tilde{\delta}_1, \dots, \tilde{\delta}_n) \in \mathbb{R}_+^n$ viewed in polar coordinates correspond to directions to the origin in z -coordinates. Indeed, there is a bijection between these $\tilde{\delta}$ -directions, and the points on the sphere $\Psi \in S^{n-1}$ with non-negative coordinates for the blown-up z -coordinates. In terms of the z -coordinates, the real projectivized flow near $z = 0$ corresponds to the above flow on this part of the sphere, which can be related with Grassmannian linear dynamics in $z = 0$, i.e., for asymptotically large distances. However, we do not pursue this viewpoint here; the interested reader is referred to, e.g., [24,32] and the references therein.

3.2.3 Unperturbed Polar System, Part I: Radial and Angular Dynamics

Since all distances are positive, we consider the part of the sphere with positive coordinates,

$$S^+ := S^+(n) := \{x = (x_1, x_2, \dots, x_n)^T \in S^{n-1} : x_i > 0 \forall i\},$$

on which the following holds.

Proposition 6 $\Sigma_n > 0$ on $\overline{S^+}$. More specifically, $\Sigma_n > \Psi_{j_0}^2/2$, where the index j_0 is such that $\Psi_k = 0$ for $1 \leq k < j_0$ and $\Psi_k > 0$ for $j_0 \leq k \leq n$.

Note that the index j_0 exists since $(\Psi_1, \dots, \Psi_n) \in S^{n-1}$ does not vanish.

Proof Rewrite Σ_n as $\Sigma_n = \Psi_{j_0}^3 + \sum_{k=j_0+1}^n \Psi_k^2 (\Psi_k - \Psi_{k-1})$ and set $f_{k-1}(\Psi_k) := \Psi_k^2 (\Psi_k - \Psi_{k-1})$ as a function in Ψ_k with parameter Ψ_{k-1} which has its minimum (on $[0, 1]$) at $\frac{2}{3}\Psi_{k-1}$, i.e. $f_{k-1}(\Psi_k) \geq f_{k-1}(\frac{2}{3}\Psi_{k-1}) = -\frac{4}{27}\Psi_{k-1}^3$. Hence,

$$\Sigma_n \geq \Psi_{j_0}^3 - \frac{4}{27} \sum_{k=j_0+1}^n \Psi_{k-1}^3 = \Psi_{j_0}^3 - \frac{4}{27} \sum_{k=j_0}^{n-1} \Psi_k^3, \quad \Psi_k = \frac{2}{3}\Psi_{k-1}. \tag{28}$$

Since $\Psi_k = \frac{2}{3}\Psi_{k-1}$ one gets $\Psi_k = \left(\frac{2}{3}\right)^{k-j_0} \Psi_{j_0}$ by recursion and consequently,

$$\Sigma_n \geq \Psi_{j_0}^3 - \frac{4}{27} \sum_{k=j_0}^{n-1} \left(\frac{2}{3}\right)^{3(k-j_0)} \Psi_{j_0}^3 > \Psi_{j_0}^3 \left(1 - \frac{4}{27} \sum_{k=0}^{\infty} \left(\frac{2}{3}\right)^k\right) = \frac{15}{27} \Psi_{j_0}^3 > \frac{1}{2} \Psi_{j_0}^3$$

□

Lemma 2 $\Psi'_j > 0$ for $0 < \Psi_j \ll 1$ and there exist $T > 0, \varepsilon > 0$ such that $\Psi_j(t) \in (\varepsilon, 1 - \varepsilon)$ for all $t \geq T$.

Proof If $\Psi_j = 0$, we have $\Psi_{j-1} - \Psi_j + \Sigma_n = \Psi_{j-1} + \Sigma_n > 0$. Choosing $\Psi_j > 0$ small enough, we therefore get $\Psi'_j = \Psi_j(\Psi_{j-1} - \Psi_j + \Sigma_n) > 0$. This, together with Proposition 6, implies the second statement by contradiction. □

As a consequence, the distances of the distances $\tilde{\delta}_j$ in the unperturbed ODE system are bounded.

Proposition 7 Solutions to (20) satisfy $|\tilde{\delta}_j - \tilde{\delta}_k| > 0$ and $\tilde{\delta}_j - \tilde{\delta}_k = \mathcal{O}(1)$ as $t \rightarrow \infty$.

Proof The distances are eventually ordered (cf. Theorem 4), thus $|\tilde{\delta}_j - \tilde{\delta}_k| > 0$ for large $t > 0$. To prove the boundedness, suppose that $\tilde{\delta}_j - \tilde{\delta}_k \rightarrow \infty$. Then, $e^{-(\tilde{\delta}_j - \tilde{\delta}_k)} = \frac{z_j}{z_k} = \frac{\Psi_j}{\Psi_k} \rightarrow 0$. However, due to Lemma 2, $\frac{\Psi_j}{\Psi_k} \in \left(\frac{\varepsilon}{1-\varepsilon}, \frac{1-\varepsilon}{\varepsilon}\right)$ for large $t > 0$. □

3.2.4 Consequences for the Perturbed Polar System

We now return to the system (23)–(25). On the sphere (i.e. for $r = 0$), the angular equations (24) and (25) coincide with those of the unperturbed polar system (27). Likewise, near the sphere (i.e. for $0 < r \ll 1$), the radial dynamics (23) are dominated by the radial term $-\Sigma_n r$, cf. (26). This allows for a perturbation argument from which one can deduce that the distances in the perturbed system diverge.

Theorem 5 There is $\tilde{\delta}_0 > 0$ such for all solutions to (19) with $\tilde{\delta}_{\min}(0) > \tilde{\delta}_0$, the statements of Theorem 4 and Proposition 7 hold true. In particular, there exists $\tilde{\delta}_1 \geq 0$ such that for all solutions to (19) with $\tilde{\delta}_{\min}(0) > \tilde{\delta}_1$ it holds that $\tilde{\delta}_{\min}(t) \geq \tilde{\delta}_{\min}(0)$ for all $t \geq 0$.

Note that together with Proposition 5 this in particular implies Theorem 3.

Proof With respect to the unperturbed polar system (26)–(27), $\mathcal{M}_0 := \{r = 0\} \times S^+$ is an inflowing normally hyperbolic invariant manifold (cf. [29,52]) since the transversal eigenvalues are strictly negative, cf. Proposition 6, and the boundary is repulsive due to Lemma 2. By robustness of such invariant manifolds, \mathcal{M}_0 possesses a non-trivial local basin of attraction Γ for the unperturbed and perturbed polar systems (23)–(25). Theorem 4 implies that any solution to the unperturbed system with angular initial data in S^+ enters Γ in finite time, which therefore also holds for the perturbed system if initial distances are sufficiently large. These solutions thus converge to \mathcal{M}_0 . The property that eventually $\Psi_j \in (\varepsilon, 1 - \varepsilon)$, cf. Lemma 2, is likewise structurally stable and thus remains valid for the perturbed polar system. In particular, this property means that all distances $\tilde{\delta}_j$ diverge.

Without loss of generality, we can choose Γ to lie in the n -dimensional local stable manifold W^s of \mathcal{M}_0 in the unperturbed system, which we write as $W^s(S^+)$ since \mathcal{M}_0 is

trivially parameterized by S^+ . Now, for the perturbed and unperturbed polar system, $W^s(S^+)$ is foliated by one-dimensional strong stable fibers $W^{ss}(\Psi)$, respectively,

$$W^s(S^+) = \bigcup_{\Psi \in S^+} W^{ss}(\Psi), \tag{29}$$

which are pairwise disjoint and each intersect \mathcal{M}_0 in their base point $\Psi \in S^+$. The dynamics of the base points is given by (27) for both the perturbed and unperturbed polar systems, but the fibers differ in general.

The key point is that the flows of both (26)–(27) and (23)–(25) in Γ are slaved to the base point flow such that the perturbed flow inherits the properties of the unperturbed flow as claimed. More specifically, let $\Psi(t), \Psi(0) \in S^+$ be a solution to (27). Then the perturbed and unperturbed flows map their respective fibre $W^{ss}(\Psi(0))$ into their respective fibre $W^{ss}(\Psi(t))$; using the foliation (29) for local coordinates of the perturbed system near the sphere, the base flow (which is always the same) decouples from the transverse fibre flow, which differs between perturbed and unperturbed flow.

Since the base point flow leads to an eventually ordering of the distances for the unperturbed polar system, cf. Theorem 4, the slaving implies the same for the perturbed system (19). The remaining claims follow analogously. These imply that there is $\tilde{\delta}_*$ such that $\tilde{\delta}_{\min}(t)$ grows strictly if $\tilde{\delta}_{\min} \geq \tilde{\delta}_*$, which implies the existence of an $\tilde{\delta}_1 \leq \tilde{\delta}_*$ as claimed. \square

3.2.5 Unperturbed Polar System, Part II: Local Stability

Here we add more details to the dynamics of the unperturbed polar system: we prove that there is a unique equilibrium point in S^+ , and it is locally exponentially stable. For illustration, let us first consider the simplest cases $n = 2$ and $n = 3$, cf. Fig. 5.

For $n = 2$, the system (27), with $\Sigma_2 = \Psi_1^3 - \Psi_1\Psi_2^2 + \Psi_2^3$, reads

$$\begin{aligned} \Psi_1' &= \Psi_1(-\Psi_1 + \Sigma_2) \\ \Psi_2' &= \Psi_2(\Psi_1 - \Psi_2 + \Sigma_2). \end{aligned}$$

Let us first assume that $\Psi_1 \neq 0$ which implies $\Psi_1 = \Sigma_2$ for an equilibrium. If $\Psi_2 \neq 0$, then $\Psi_2 = 2\Psi_1$ and thus $\Psi_1 = \pm\sqrt{\frac{1}{5}}$, and yields the two equilibria $E_{1,2} := \pm\left(\sqrt{\frac{1}{5}}, 2\sqrt{\frac{1}{5}}\right)$.

For $\Phi_2 = 0$ we find the two equilibria $E_{3,4} := (\pm 1, 0)$ and for $\Phi_1 = 0$ the last two, $E_{5,6} := (0, \pm 1)$. In total, the system has $S_2 := 2(2^2 - 1) = 6$ equilibria.

For $n = 3$, the situation is already a bit more complicated. We have $\Sigma_3 = \Psi_1^3 - \Psi_1\Psi_2^2 + \Psi_2^3 - \Psi_2\Psi_3^2 + \Psi_3^3$ and need to distinguish the following different cases depending on the number $0 \leq k \leq 2$ of zero coordinates, each giving a pair of equilibria:

- (i) $k = 0 : E_{1,2} = \pm\left(\sqrt{\frac{1}{14}}, 2\sqrt{\frac{1}{14}}, 3\sqrt{\frac{1}{14}}\right)$
- (ii) $k = 1 : E_{3,4} = \pm\left(\sqrt{\frac{1}{5}}, 2\sqrt{\frac{1}{5}}, 0\right), E_{5,6} = \pm\left(\sqrt{\frac{1}{2}}, 0, \sqrt{\frac{1}{2}}\right), E_{7,8} = \pm\left(0, \sqrt{\frac{1}{5}}, 2\sqrt{\frac{1}{5}}\right)$
- (iii) $k = 2 : E_{9,10} = (\pm 1, 0, 0), E_{11,12} = (0, \pm 1, 0), E_{13,14} = (0, 0, \pm 1)$

In total, the system has $S_3 := 2(2^3 - 1) = 14$ equilibria.

For general $n \in \mathbb{N}$ the following holds.

Proposition 8 *For $n \in \mathbb{N}$, system (27) possesses $S_n := 2(2^n - 1)$ equilibria. Specifically, there are (i) $2n$ equilibria which have exactly one non-zero component (which is therefore ± 1) and (ii) $S_n - 2n - 2$ equilibria with $2 \leq j \leq n - 1$ non-zero components.*

Proof Let $n \in \mathbb{N}$ and S_n denote the number of equilibria $\Psi = (\Psi_1, \dots, \Psi_n)$ of dimension n . First note that $\Psi_j \neq 0$ implies for equilibria $\Psi_j = \Sigma_n + \Psi_{j-1}$ by (27). Thus, $\Psi_{j-1} = 0, \Psi_j \neq 0$ implies $\Psi_j = \Sigma_n$, and adjacent non-zero entries come as a sequence $(\Sigma_n, 2\Sigma_n, \dots, k\Sigma_n)$, where $2 \leq k \leq n$. Hence, an intermediate zero coordinate between two non-zero coordinates results in a triple $(\Sigma_n, 0, \Sigma_n)$.

Consequently, if $\Psi_1 = 0$, the S_{n-1} equilibria of dimension $n - 1$ occur with shifted index; this in particular includes the vectors with $\Psi_j = \pm 1$ for some $2 \leq j \leq n$ and zero coordinates otherwise. Denote the number of remaining equilibria with $\Psi_1 \neq 0$ by M_n . By the discussion above, M_n is the number of possibilities to have $k \in \{0, 1, \dots, n - 1\}$ zero entries on the positions different from $\Psi_1 \neq 0$ (in particular including $(\pm 1, 0, 0, \dots, 0)$). This number is given by $M_n = 2 \sum_{k=0}^{n-1} \binom{n-1}{k}$.

All together,

$$S_n = M_n + S_{n-1} = \sum_{j=1}^n M_j = 2 \sum_{j=1}^n \sum_{k=0}^{j-1} \binom{j-1}{k} = 2 \sum_{j=1}^n 2^{j-1} = 2(2^n - 1).$$

□

By the previous lemma, the unique equilibria with non-zero coordinates only are given by $E_{\pm} := (\Psi_1, 2\Psi_1, 3\Psi_1, \dots, n\Psi_1)$, where $\Psi_1 = \pm \sqrt{\frac{6}{n(n+1)(2n+1)}}$.

Local stability of E_+ . In the following, we focus on $E := E_+$ since for the question of divergence of the distances in the perturbed ODE-system this is the only relevant asymptotic state. In fact, we expect that it is a global attractor on S^+ as can be illustrated by simulations for $n = 2$ and $n = 3$, cf. Fig. 5. However, it seems difficult to prove this rigorously in general. Instead, by linearizing (27) in E and determining the eigenvalues of the Jacobian, we show that E is locally stable on S^{n-1} .

Theorem 6 *The equilibrium E is locally exponentially stable on S^{n-1} . The eigenvalues of the linearisation in E are given by $-\frac{k}{6}n(n+1)(2n+1), 2 \leq k \leq n$. For the full unperturbed polar system in \mathbb{R}^n , E possesses the unstable eigendirection transverse to \mathcal{M}_0 spanned by $(1, 2, \dots, n)^T$ with corresponding eigenvalue $\frac{1}{3}n(n+1)(2n+1)$.*

Proof The somewhat lengthy proof is given in “Appendix B”. □

4 Bounded Initial Kink-Antikink Data and their Annihilation

Having discussed pure kink or antikink initial data, we now turn to initial data which are composed of kinks and antikinks, that is, initial data (5) with $n + m < \infty$ and $nm \neq 0$, cf. Fig. 6 for illustration. Here we constrain ourselves to bounded data and consider the unbounded case in Sect. 5. We aim to infer information about the process by which the respective inner pair of kink and antikink with positions $\xi_1^{\pm}(t)$ annihilate each other.

4.1 Annihilation Process

In case $m = n$, the equal number of pairs of kinks and antikinks completely annihilate each other in the sense that the solution converges to the rest state $2\pi n$ given by the asymptotic state of the initial data.

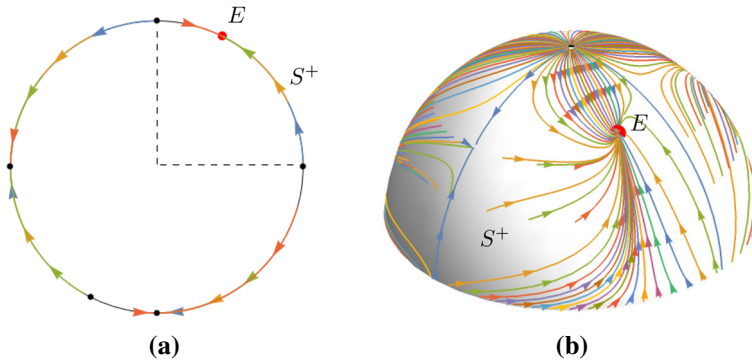
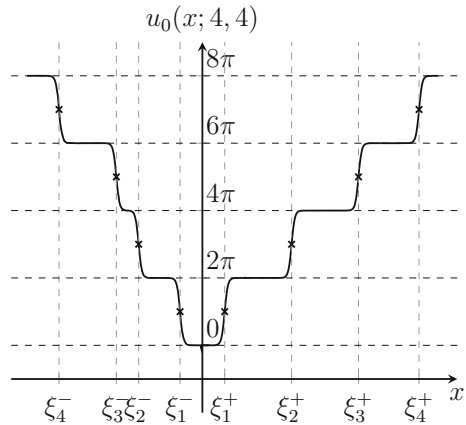


Fig. 5 Phase portraits and equilibrium E (marked as red point) for **a** $n = 2$ and **b** $n = 3$, respectively. For better visibility, the phase portrait is restricted to the upper hemisphere for $n = 3$. As these simulations suggest, E is a global attractor on S^+ for these cases

Fig. 6 Sketch of initial datum (5) with $m = n = 4$



Proposition 9 Let $u_0(x, n, n)$ be an initial datum (5) with $m = n, 0 < n < \infty$. Then, $\lim_{t \rightarrow \infty} u(\cdot, t) = 2\pi n$, where the convergence is uniform in $x \in \mathbb{R}$. In particular, $\omega(u_0(x; n)) = \Omega(u_0(x; n)) = \{2\pi n\}$.

Proof Consider subsolutions with initial data the pure kink- or antikink sequence $u_0(x; n, 0), u_0(x; 0, n)$ built from the kink- or antikink positions of $u_0(x; n, n)$, respectively. According to Theorem 1.1 [39] the kinks and antikinks move with uniform positive, respectively negative speed. The comparison principle implies the claim. \square

The following proposition describes the corresponding annihilation process in some more detail by showing that the kinks-antikink pairs get annihilated successively from “bottom to top” as expected intuitively.

Proposition 10 Let $u_0(x; n, n)$ be an initial datum (5) with $n < \infty$ and corresponding solution $u(x, t)$. Then, there are unique times $0 < t_1 < t_2 < \dots < t_n$ such that $\xi_j^-(t_j) = \xi_i^+(t_j), 1 \leq j \leq n$, i.e., the successively innermost kink and antikink collide at these times. Moreover, there are unique times $t_j^A \in (t_j, t_{j+1}), 1 \leq j \leq n - 1$, such that $\operatorname{argmin}_{x \in \mathbb{R}} \{u(x, t_j^A)\} = 2\pi j$, i.e., at these times the successively innermost kink and antikink annihilate.

To ease notation we set $t_0^A := 0$.

Proof As shown in the proof of Proposition 1, for all $t > 0$, the solution $u(x, t)$ is monotonically decreasing on $(-\infty, \eta(t))$ with $\lim_{x \rightarrow -\infty} u(x, t) = 2\pi n$ and monotonically increasing on $(\eta(t), \infty)$ with $\lim_{x \rightarrow \infty} u(x, t) = 2\pi n$. Together with Proposition 9, this shows that the positions $\xi_i^\pm(t)$, $1 \leq i \leq n$, collide at some unique time $t_i > 0$, respectively, i.e., $u(\eta(t_i), t_i) = (2i - 1)\pi$ and $u(\cdot, t; n) > (2i - 1)\pi$ for $t > t_i$; therefore $\xi_i^\pm(t)$ exist for $[0, t_i]$ only. In particular, $t_i < t_{i+1}$. Analogously, we identify the annihilation times $t_i^A \in (t_i, t_{i+1})$. \square

Next we show that during the annihilation process of the innermost kink-antikink pair, the distances between the remaining kinks (antikinks) satisfy a uniform lower bound.

Proposition 11 *Let $u(x, t)$ be the solution corresponding to an initial condition as above. Then, $d_j^\pm(t) \geq d_{\min}^\pm(0)$ and if j^\pm are indices such that $d_{\min}^\pm(0) = d_{j^\pm}(0)$ then $d_{j^\pm}(t)$ are non-decreasing as long as defined, i.e., $t \leq t_j$, respectively. In particular, $|\xi_{j+1}^-(t) - \xi_{j+1}^+(t)| \geq d_{\min}^+(0) + d_{\min}^-(0) + |\xi_j^-(t) - \xi_j^+(t)|$ for all $t \in (0, t_j]$.*

Proof Due to reflection symmetry, it suffices to prove the claims for the case ‘+’. In the proof of Proposition 3, we have constructed initial conditions \underline{u}_0 and \bar{u}_0 whose corresponding solutions $\underline{u}(x, t)$, $\bar{u}(x, t)$ are sub- and supersolutions, which imply the non-decrease of the minimal distance. In the present case the same subsolutions can be used. However, \bar{u}_0 are not providing supersolutions on \mathbb{R} , but only on $(-\infty, \eta(t))$ since $u(\cdot, t)$ is minimal at $\eta(t)$ and $\bar{u}(x, t)$ can be above $u(x, t)$ only for $x > \eta(t)$. The claims now follow from the statement of Proposition 3. \square

It is tempting to suppose that the minimal distance between kinks or antikinks, respectively, that arises after annihilations can be used as a lower bound. However, it seems difficult to construct super- and subsolutions to substantiate this.

Let us now turn to the case of initial data with unequal number of kinks and antikinks, $m \neq n$; without loss of generality $m < n$. In this situation, the first $\min\{m, n\}$ innermost kink-antikink pairs annihilate and a stacked front of either kinks or antikinks remains after some finite time.

Proposition 12 *Let $u_0(x; m, n)$ be an initial datum (5) with $m < n < \infty$ and $mn \neq 0$. The kinks and antikinks at $\xi_i^\pm(t)$, $1 \leq i \leq m$, collide and annihilate in the sense of Proposition 10. Moreover, the limit sets are given by*

$$\begin{aligned} \omega(u_0(x; m, n)) &= \{2\pi n\}, \\ \Omega(u_0(x; m, n)) &= \{2\pi j : m \leq j \leq n\} \cup \{\varphi_j^+(\cdot - v) : m < j < n, v \in \mathbb{R}\}. \end{aligned}$$

Proof In the course of the annihilation process of the m innermost kink-antikink pairs, $u(x, t)$ gets uniformly close to $2\pi m$ for $x \leq \eta(t)$. Meanwhile, the distances d_j^+ ($m \leq j < n$) of the remaining kinks are bounded from below by Proposition 11, which means the solution gets arbitrarily close to a propagating terrace. Since $2\pi m$ is a stable steady state, the solution $u(x, t)$ converges to a propagating terrace and [39, Theorem 1.1] implies the statement. \square

Towards a more complete picture, let us briefly consider initial data with local maxima built by pairs of kinks and antikinks, cf. Fig. 7. For each such maximum with sufficiently large distance of kink and antikink, one can construct a stationary subsolution using phase plane analysis for the equation $u_{xx} + f(u) = 0$; this shows that kinks and antikinks cannot annihilate at local maxima, but only between local minima as described before. In particular, the limit sets $\omega(u_0)$ and $\Omega(u_0)$ are completely determined by the numbers m, n between maxima.

Fig. 7 Sketch of initial datum with local maximum and subsolution (red). Kink and antikink which built the local maximum cannot collide

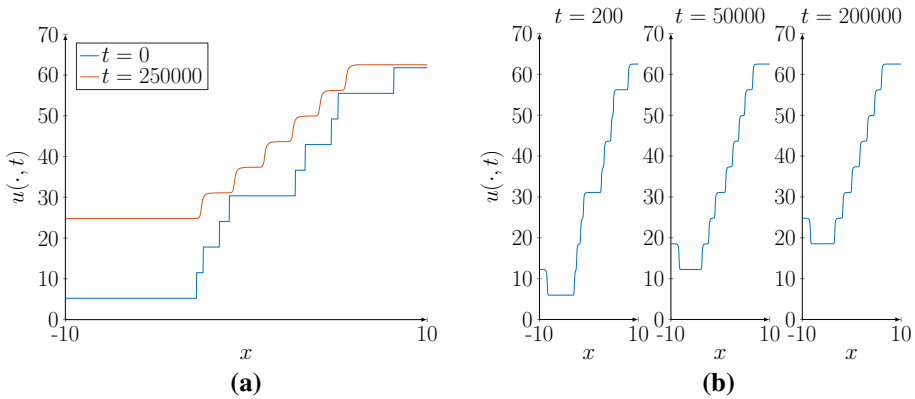
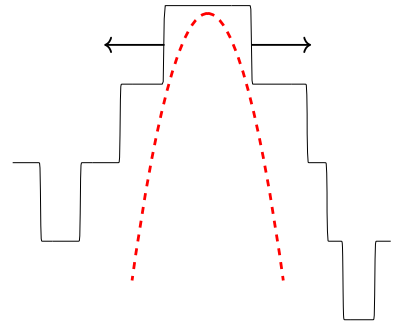


Fig. 8 Simulations to illustrate the loss of information ($f_0 = 0.2$). **a** Information encoded in the initial kink distances is locally “washed out” at $t = 250,000$, independent of three ‘fast’ annihilations due to incoming kinks as plotted in **(b)**. Here the initial datum is composed of antikinks only and the incoming kinks are artificially generated at later times by changing the boundary values; this avoids otherwise prohibitively expansive numerics as one can use a small spatial domain to catch both the slow weak interaction and the much faster pulse motion. See “Appendix C” for details on the implementation

5 Unbounded Kink or Kink-Antikink Data

Unbounded initial data is most relevant for the comparison with the dynamics of the cellular automaton GHCA, such as its non-wandering set dynamics and topological entropy. However, for unbounded data several useful results cannot be directly applied, e.g., those on terraces in [39].

Nevertheless, the zero number argument is still applicable (the growth condition of [4, p. 80] is satisfied for $u \in X_\omega$) so that we readily infer an analogue to Proposition 10 in case $m = n = \infty$: we can repeatedly choose initial data composed of finite kink-antikink pairs as subsolutions and obtain an infinite sequence of strictly increasing collision and annihilation times.

However, numerical simulations of (1) (lifted to $u(x, t) \in \mathbb{R}$), cf. Figs. 8, 9, suggest that distances equilibrate asymptotically in time. Hence, initial distance information encoded far from an eventual collision is lost over time, is “washed out”—at least on the scale of the initial data. Indeed, this is consistent with our results on the dynamics of analytic positions for monotone data, and large initial distances. Therefore, as suspected from weak interaction

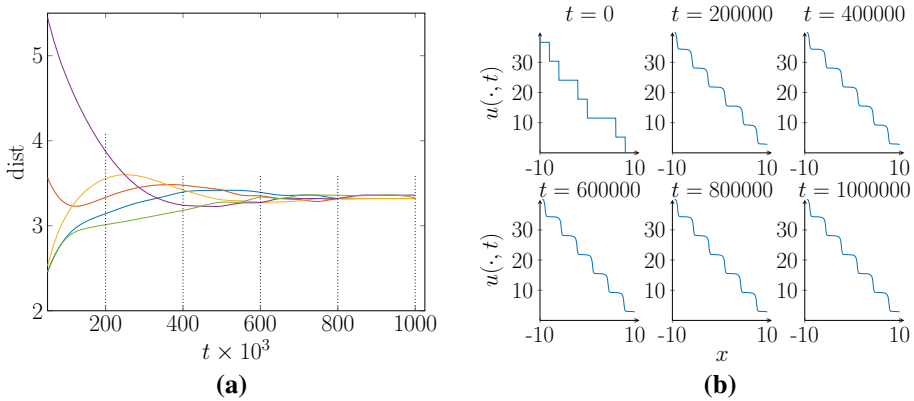


Fig. 9 Simulation of **a** kink distances and **b** corresponding solutions done with pde2path by freezing under periodic boundary conditions and with $f_0 = 0.2$, cf. “Appendix C”. The initial datum converges to an equidistant state

induced by diffusion, we cannot expect entropy and dynamics for (1) with unbounded initial data are directly analogous to GHCA.

We first corroborate the equilibration of distances for unbounded initial data by considering periodic boundary conditions and show that all solutions converge locally uniformly to equidistant staircases. Second, we discuss implications for complexity measures based on positional dynamics.

5.1 Periodic Boundary Conditions

Unbounded superpositions of equidistant kinks (and, analogously, antikinks) are parametrized by the uniform distance $\ell > 0$, and the problem is transformed into a boundary value problem under periodic boundary conditions, up to phase rotation.

More precisely, for given $\ell \in \mathbb{R}_+$ and $j \in \mathbb{N}$, we consider the initial-boundary value problem

$$\begin{cases} \theta_t = \theta_{xx} + f(\theta), & -\ell \leq x \leq \ell & (30a) \\ \theta(0, x) = \theta_0(x), & -\ell \leq x \leq \ell & (30b) \\ \theta(-\ell) = \theta(\ell) + 2\pi j, & \theta(-\ell) \leq \theta \leq \theta(\ell) & (30c) \\ \theta'(-\ell) = \theta'(\ell) & & (30d) \end{cases}$$

and prove in Proposition 15 below that solutions of (30) converge to a unique equidistant staircase in terms of the ω -limit set of θ_0 .

To this end, we first consider travelling wave solutions $\theta(x, t) = u(x - at) =: u(z)$ and focus on the following boundary value problem, where $' = \frac{d}{dz}$.

Proposition 13 For each triple $(\ell, j, a) \in \mathbb{R}^+ \times \mathbb{N} \times \mathbb{R}$, the boundary value problem

$$\begin{cases} u'' + au' + f(u) = 0, & -\ell < x < \ell & (31a) \\ u(-\ell) = 2\pi j, u(\ell) = 0, & 0 \leq u \leq 2\pi j & (31b) \end{cases}$$

has a unique, monotonously decreasing solution u with $\partial_x u < 0$ on $(-\ell, \ell)$. Moreover, there exists a unique $a(\ell, j)$ such that the unique solution u of (31) corresponding to $(\ell, j, a(\ell, j))$

additionally satisfies $u'(-\ell) = u'(\ell)$. This $a(\ell, j)$ is given by

$$a(\ell, j) = (F(2\pi j) - F(0)) \left(\int_{-\ell}^{\ell} (u')^2 dx \right)^{-1},$$

where $F' = f$. In particular, $\lim_{\ell \rightarrow 0} a(\ell, j) = 0$.

We remark that the case $j = 1$ is essentially contained in [41, Thm 3.5].

Proof Sub- and super solutions are given by $\underline{u} \equiv 0$ and $\bar{u} \equiv 2\pi j$, respectively, which shows the existence of a solution u . Applying Theorem 1.4 [5] (“sliding method”) to $\Omega_\ell := [-\ell, \ell]$, together with the maximum principle, implies the monotonicity and uniqueness of this solution.

Moreover, this unique solution (i) depends continuously on a and (ii) is strictly decreasing in its dependence on a (i.e. if $a_1 < a_2$, then $u_2 < u_1$ in Ω_ℓ , where u_1 and u_2 are the solutions of (31) corresponding to (ℓ, j, a_i) , $i = 1, 2$, cf. Corollary 5.1 [6]). By Lemma 5.2 [6], one infers that (iii) $\lim_{a \rightarrow -\infty} u = 2\pi j$ and $\lim_{a \rightarrow \infty} u = 0$, both uniformly in x . Items (i)-(iii) together imply the existence of a unique solution u and a unique $a(\ell, j)$ such that $u'(-\ell) = u'(\ell)$.

As to $a(\ell, j)$ and its asymptotics, one multiplies equation (31a) by u' and integrates to get

$$a(\ell, j) \int_{-\ell}^{\ell} (u')^2 dx = - \int_{-\ell}^{\ell} u' u'' + u' f(u) dx = F(2\pi j) - F(0),$$

where $u'(-\ell) = u'(\ell)$ is used. We obtain $a(\ell, j) = (F(2\pi j) - F(0)) \left(\int_{-\ell}^{\ell} (u')^2 dx \right)^{-1}$. By the Cauchy-Schwarz inequality,

$$\int_{-\ell}^{\ell} (u')^2 dx \geq \frac{4\pi^2 j^2}{2\ell}$$

and thus $a(\ell, j) \rightarrow 0$ as $\ell \rightarrow 0$. □

Remark 5 Since f is 2π -periodic, the statement clearly remains true for boundary conditions $u(\ell) = 2\pi k$ and $u(-\ell) = 2\pi(k + j)$, $j, k \in \mathbb{N}$, and the solution is just $u + 2\pi k$; in particular (30c), (30d) hold. We also remark that $F(2\pi j) \neq F(0)$ for our nonlinearity f .

In the following, we focus on the unique solution u of (31) corresponding to the triple $(\ell, j, a(\ell, j))$. Due to its additional property $u'(-\ell) = u'(\ell)$, it is the relevant solution for the purposes of this section. As a consequence of the previous proposition, its shape is determined by single periodic solutions in the following sense; in particular all kinks in u are equidistant.

Proposition 14 *Let u denote the unique solution of (31) which corresponds to the triple $(\ell, j, a(\ell, j))$. Then u consists of j space shifted and phase rotated copies of the solution \tilde{u} of (31) corresponding to $(\tilde{\ell}, 1, a(\tilde{\ell}, 1))$ with $\tilde{\ell} = \ell/j$. In particular, $a(\ell, j) = a(\tilde{\ell}, 1)$, $u'(\pm\ell) = \tilde{u}'(\pm\tilde{\ell}) < 0$ and u has time period $T = \tilde{\ell}/a(\tilde{\ell}, 1)$.*

Proof We split the interval $[-\ell, \ell]$ into j intervals $I_s := [\ell_{s+1}, \ell_s]$, $(0 \leq s \leq j - 1)$ of width $2\tilde{\ell}$, where $\ell_s := \ell - 2s\tilde{\ell}$. In particular, $\ell_s > \ell_{s+1}$ and $\ell_0 = \ell, \ell_j = -\ell$. On each interval, we consider a space shifted and phase rotated version of \tilde{u} which together build a solution due to equal derivatives at the boundaries. More precisely, let $v(x) := \tilde{u}(x - (j - 1)\tilde{\ell})$ be the spatial shift of \tilde{u} to the rightmost interval I_0 and, for $s \in \{0, 1 \dots j - 1\}$, set

$$U(x) := v(x + 2s\tilde{\ell}) + 2\pi s, \quad x \in I_s.$$

The function U is thus defined on $[-\ell, \ell]$ and solves (31) with $a = a(\tilde{\ell}, 1)$ and, moreover, $U'(-\ell) = U'(\ell)$. By the uniqueness result of Proposition 13, it follows that $U = u$ and, in particular, $a(\ell, j) = a(\tilde{\ell}, 1)$ and $u'(\pm\ell) = \tilde{u}'(\pm\tilde{\ell})$. By the construction of U , the same proposition implies $\tilde{u}'(\pm\tilde{\ell}) < 0$ since $u'(x) < 0$ for all $x \in (-\ell, \ell)$. \square

Having established the unique solution of problem (31) with $u'(-\ell) = u'(\ell)$, we next show that solutions of (30) converge to this solutions in the following sense; without loss of generality, we choose $\theta(\ell) = 0$ and consider continuous initial conditions $0 \leq \theta_0 \leq 2\pi j, j \in \mathbb{N}$.

Proposition 15 *Let u be a solution of rm (30) with $\theta(\ell) = 0$ and initial datum $0 \leq \theta_0 \leq 2\pi j$ for some $j \in \mathbb{N}$. Then, the ω -limit set of θ_0 consists of the orbit associated to the unique solution of (31) corresponding to $(\ell, j, a(\ell, j))$.*

Proof This is basically a consequence of [22, Theorem 1] which characterises the limit set by providing a dichotomy between stationary and periodic solutions. However, in order to apply this theorem, we need to transform (30) into a problem with periodic boundary conditions.

To this end, we consider $w(x, t) := \theta(x, t) + \frac{\pi j(x-\ell)}{\ell}$ which transforms the problem into

$$\begin{cases} w_t = w_{xx} + g(x, w), & (32a) \\ w(0, x) = w_0(x) = \theta_0(x) + \frac{\pi j(x-\ell)}{\ell}, & (32b) \\ w(-\ell) = w(-\ell), & (32c) \\ w'(-\ell) = w'(\ell) & (32d) \end{cases}$$

where $g(x, w) := f\left(w - \frac{\pi j(x-\ell)}{\ell}\right)$. In particular, there is a one-to-one relation between solutions of (30) and (32). Let \hat{u} denote the unique solution of (31) associated with $(\ell, j, a(\ell, j))$. Since $W(x, t) = \hat{u}(x - a(\ell)t) + \frac{\pi j(x-\ell)}{\ell}$ is a periodic solution solution of (32), the mentioned dichotomy implies that $\omega(w_0)$ consists of the periodic orbit associated with W and transforming back proves the statement. \square

Remark 6 The previous proposition shows that solutions of (30) converge locally uniformly to (some translate of) the corresponding unique solution of (31), i.e., the kinks become equidistant, cf. Fig. 9. For a general analysis of convergence in one-dimensional semilinear heat equations, including other types of boundary conditions and nonlinearities, we refer to [1,12,35] and references therein.

5.2 Complexity Considerations

The motivation to consider kink-antikink dynamics in the θ -equations emerges from our analysis of GHCA and their (topological) complexity [31]. The understanding of this complexity mainly relies on the observation that for GHCA the original and somehow abstract definitions of topological entropy [3,7] can be substantiated by considering simpler but equivalent definitions. In this regard, one combinatorial approach is to count the number $W_{m,n}$ of possible realizations of the dynamics on bounded space-time windows $[-m, m] \times [0, n - 1]$, where $m \in \mathbb{Z}, n \in \mathbb{N}$, and to determine the exponential growth rate of $W_{m,n}$ as the size of these windows increases [16,31]. On the other hand, the decomposition of the non-wandering set reveals that the topological complexity is completely determined by the invariant subsystem consisting of bi-infinite configurations which are composed of counter propagating pulses,

$$(\dots, 0_{k_j}, w^R, 0_{k_{j+1}}, \dots, w^R, 0_{k_0}, w^L, 0_{k_1}, w^L, \dots), \tag{33}$$

where $0_k : (0, \dots, 0)$ are zero blocks of length $k \in \mathbb{N}$ and $w^{R,L}$ represent local pulses, i.e., blocks that move to the right and left under the CA-dynamics, respectively. Thus, a more tailored way to encode the topological complexity of GHCA relies on the construction of a topological conjugacy by defining a proper homeomorphism that maps counter propagating configurations to admissible sequences of *collision sequences* in the form of pairs $(p_n, s_n)_{n \in \mathbb{N}} \subset \mathbb{Z} \times \mathbb{N}$ of collision positions p_n and times s_n .

We stress that the consistency of these two approaches to determine the topological entropy is crucially based on the specific dynamics and topological setup of GHCA and is far from general validity.

Nevertheless, for θ -equations, tracking the geometric or analytic kink and antikink positions provides a mapping from kink-antikink initial data to collision sequences and thus allows for a comparison with those of GHCA with its encoded complexity. Hence, insight into position dynamics of kink, antikink and kink-antikink initial data is a prerequisite for at least a first heuristic insight into the underlying complexity of the dynamics

As we have shown, bounded initial data give finite sequences of this kind, but for unequal numbers of kinks and antikinks the positional dynamics remains non-trivial also after the final collision in terms of terraces. This eventually occurs on an exponentially slow time scale and distances of terraces eventually diverge, cf. Propositions 2–3, so that we do not expect a significant contribution to any position-based complexity measure. This may be corroborated further based on our lower bounds for the distances and the ODE for large initial distances, which severely constrains the positions and thus a priori reduces a position based complexity. This metastable slow dynamics already occurs before collisions and thus modifies the relation of initial positions and collision sequence. However, this is a perturbation for any fixed number of n initial kinks and antikinks, and we conjecture this can be compensated by a perturbation of initial positions.

In contrast, the above result on equilibration of distances strongly suggest that this is no longer true for unbounded kink-antikink initial data. While the dynamics of (semi-)unbounded kink or antikink data resembles the pure shift dynamics of (semi-)infinite pulse configurations of GHCA, the dynamics of unbounded kink-antikink data bears resemblance to that of infinite counter propagating pulses of GHCA—up to the aforementioned equilibration of distances for ‘late’ collisions.

For a direct comparison to the complexity of GHCA in terms of positions, a more specific question is whether any given admissible sequence of collision positions and times for GHCA can also be realized by appropriate initial kink-antikink data. To be more concrete, let $x = (x_n)_{n \in \mathbb{Z}}$ denote a configuration of the form (33) with pulse positions p_i^- (right-moving) and p_i^+ (left-moving), respectively, which realizes a given sequence $(p_n, s_n)_{n \in \mathbb{N}}$ of collision points and times. On the one hand, if we choose kink and antikink positions to be exactly the same, $\xi_i^\pm = p_i^\pm$, in general one cannot expect to observe the given collisions positions and times (cf. “washing out”, Fig. 8). On the other hand, this does not rule out the possibility that a time-rescaled sequence $(p_n, \tau s_n)_{n \in \mathbb{N}}$, with suitable scaling factor τ , can be attained from modified initial kink and antikink positions, especially because the equilibration of distances is a phenomenon under large distances, i.e., far from collisions only. This shows that more general quantitative knowledge about the position dynamics, including less restrictive initial data, is required in order to analyze these aspects rigorously.

6 Discussion

Motivated by studies of the Greenberg-Hastings cellular automaton (GHCA) as a caricature of excitable systems, in this paper we have considered the θ -equations describing oscillatory phase dynamics, as the perhaps simplest PDE model of excitable media. Since the non-wandering set of GHCA in essence consists of certain excitation pulse sequences [31], we have focussed on the analogue of such data in θ -equations, which consists of kinks and antikinks. Moreover, in GHCA the topological entropy can be related to kink-antikink collisions. We have therefore analyzed the dynamics of bounded and unbounded kink-antikink initial data, including pure kink and antikink data. To this end, we have defined geometric and analytic positions of kinks and antikinks, the first used for a qualitative analysis of bounded and unbounded data, the latter for quantitative results concerning bounded monotone data. For bounded initial data, the theory of terraces shows that, up to spatial reflection, the ω -limit set indeed consists essentially of finite kink-sequences that weakly interact [39,42].

As to the qualitative analysis, we have shown that the set of geometric positions is well-defined and consists of isolated points that lie on smooth curves up to collisions. Using the comparison principle, we have revealed that the minimal initial distance is a global lower bound for distances and that collision times and positions can be tracked abstractly. As a model for unbounded data far from collisions, we have considered monotone data with periodic boundary conditions and have shown that the initial distances asymptotically equilibrate. Consequently, information encoded in these distances is lost over time which indicates that for the PDE, contrary to GHCA, an analogous topological entropy based on positions alone cannot be expected.

As a quantitative analysis, for bounded monotone data, we have derived ODE for the analytic positions of the kinks (antikinks) within the weak interaction regime. By blow-up type singular rescaling and a perturbation argument, we have shown that the dynamics is slaved to spherical dynamics and distances become ordered in finite time, and eventually diverge; again, this incorporates a loss of information in terms of initial distances.

The combination of comparison principle and weak interaction theory has revealed that the kink-antikink collision dynamics in the PDE is a multi-scale problem, in contrast to the single scale nature of the GHCA. The fast time scale is essentially determined by the speed of an individual kink, while the slow time scale stems from ‘tail’ interaction that is exponentially slow in the kink (or antikink) distances.

In order to combine these approaches for unbounded data, it would be interesting to study whether the approach of [54] can be used to admit infinitely many kinks (antikinks) in order to justify ODE for the positions, and whether the approach of [9,47]—which requires different speeds of the kinks (antikinks)—can be adapted to derive motion laws for non-monotone solutions from kink-antikink initial data. This might allow to estimate complexity measures adapted to the PDE context, and thus quantify the impact of the slow weak interaction on the fast collision dynamics.

Concerning models of excitable media from systems of PDE, such as the famous FitzHugh-Nagumo equations, there are two major issues. First, the interaction of excitation pulses no longer needs to be pure annihilation, but rebounds and even pulse replication is possible [11, 28,38]. Second, while weak interaction theory can be generalised to systems, the comparison principle cannot. Nevertheless, the heuristic conclusions extend to this case: weak and strong interaction yield a multi-scale problem and diffusion effects positional dynamics in a non-trivial way for infinitely many pulses, thus impacting positional complexity.

Lastly, we mention that the comparison principle has been replaced by energy methods in the Allen-Cahn and Cahn-Hilliard equations [49,51]. However, typical PDE systems of excitable media do not seem to possess an energy structure that could be exploited.

Funding Open Access funding enabled and organized by Projekt DEAL.

Declarations

Conflict of interest The authors declare that they have no conflict of interest.

Open Access This article is licensed under a Creative Commons Attribution 4.0 International License, which permits use, sharing, adaptation, distribution and reproduction in any medium or format, as long as you give appropriate credit to the original author(s) and the source, provide a link to the Creative Commons licence, and indicate if changes were made. The images or other third party material in this article are included in the article’s Creative Commons licence, unless indicated otherwise in a credit line to the material. If material is not included in the article’s Creative Commons licence and your intended use is not permitted by statutory regulation or exceeds the permitted use, you will need to obtain permission directly from the copyright holder. To view a copy of this licence, visit <http://creativecommons.org/licenses/by/4.0/>.

A Law of motion - ODE for the kink distances

This appendix is devoted to the derivation of the differential system (17). As explained in the introduction of Sect. 3.2, we follow the scheme presented in [17,43] that we adapt to our situation for the convenience of the reader.

Preliminaries We consider the parabolic problem (7), i.e. already in the moving framework $z = x - ct$. It admits a family of standing wave profiles $\{\varphi(\cdot - \xi) + 2k\pi, \xi \in \mathbb{R}, k \in \mathbb{Z}\}$, where φ is the unique standing wave of (7) connecting $2\pi = \varphi(-\infty)$ and $0 = \varphi(+\infty)$ such that $\varphi(0) = \pi$. Analyzing (3), it is a well known fact that φ satisfies

$$\varphi(z) = \begin{cases} 2\pi - a_- e^{\mu z} (1 + \mathcal{O}(e^{\gamma z})) & z < 0, \\ a_+ e^{\lambda z} (1 + \mathcal{O}(e^{-\gamma z})) & z \geq 0, \end{cases} \tag{34}$$

for positive a_-, a_+, γ , and where λ, μ are the eigenvalues of the linearized system at the asymptotic states $(\varphi, \varphi') = (0, 0)$ and $(\varphi, \varphi') = (2\pi, 0)$, cf. (16).

Linearizing (7) at these equilibria gives the same linear operator by periodicity of f given by

$$\mathcal{L} : \begin{cases} \mathcal{D}(\mathcal{L}) \subset \mathcal{X} \longrightarrow \mathcal{X} \\ v \longmapsto \partial_{zz}v + c\partial_zv + f'(\varphi)v. \end{cases} \tag{35}$$

For the purpose of our analysis, one can take $\mathcal{X} = L^2(\mathbb{R})$ and $\mathcal{D}(\mathcal{L}) = H^2(\mathbb{R})$. Due to the translation of the steady state equation, the operator \mathcal{L} has a kernel: $\mathcal{L}\varphi' = 0$. Since φ' has constant sign and considering the behavior of $f'(\varphi)$ as $z \rightarrow \pm\infty$ it follows from Sturm-Liouville theory that 0 is the largest eigenvalue of \mathcal{L} , it is simple, and isolated: $\mathcal{N}(\mathcal{L}) = \mathcal{N}(\mathcal{L}^2) = \varphi'\mathbb{R}$. It is a common result (see [46] or [44] for instance) that there exists a closed subspace $\mathcal{X}_1 \simeq \mathcal{R}(\mathcal{L})$ of \mathcal{X} such that $\mathcal{X} = \mathcal{X}_1 \oplus \mathcal{N}(\mathcal{L})$. The space \mathcal{X}_1 is the kernel of an element of the dual \mathcal{X}^* that we denote e^* , with the normalization $\langle \varphi', e^* \rangle = 1$. It is defined through the usual inner product

$$\langle \psi, e^* \rangle = \Lambda \int_{\mathbb{R}} e^{cz} \varphi'(z) \psi(z) dz, \tag{36}$$

where Λ is the normalization constant. It follows that the projection onto $\mathcal{N}(\mathcal{L})$ is given by $P\psi = \langle \psi, e^* \rangle \varphi'$.

In our situation, we are dealing with multiple fronts defined by their positions $\eta_1 > \eta_2 > \dots > \eta_n$. With a straightforward abuse of notation, we denote

$$\varphi_j = \varphi(\cdot - \eta_j), \quad \mathcal{L}_j = \partial_{zz} + c\partial_z + f'(\varphi_j), \quad e_j^* \simeq z \mapsto e^{c(z-\eta_j)} \varphi'_j(z).$$

Notice that if the η_j depend on time, so do these objects.

Projection Scheme Let us now turn to the proof of Lemma 1 and define the map

$$\Phi : \begin{cases} U \subset \mathbb{R}^n & \longrightarrow \mathbb{R}^n \\ (\eta_1, \dots, \eta_n) & \longmapsto (\langle w, e_1^* \rangle, \dots, \langle w, e_n^* \rangle) \end{cases} \tag{37}$$

where $w = v - \sum_{j=1}^n \varphi_j$. The Jacobian

$$\frac{\partial \Phi}{\partial \eta} = [\langle \varphi'_j, e_i^* \rangle - \delta_{i,j} \langle w, e^{c(z-\eta_i)} \varphi''_j \rangle]_{i,j=1}^n$$

has diagonal entries close to 1 for $0 < \varepsilon, \delta^{-1}$ small enough, i.e. w small and distances $|\eta_i - \eta_j|$ large enough, while the off-diagonal entries are close to zero. The implicit function theorem gives the desired result.

Reduced ODE We turn out to the derivation of (17). Let us emphasize once again that we refer to [17] for further details and proofs of all the underlying estimates.

To get the reduced ODE equation we use the Ansatz (8). It yields

$$\partial_t u = - \sum_{j=1}^n \eta'_j \varphi'_j + \partial_t w = L[u], \tag{38}$$

where $L[v] := \partial_{zz}v + c\partial_zv + f(v)$ denotes the nonlinear operator associated with our problem. Let us project (38) onto the kernel of \mathcal{L}_j^* , for all $j \in \{1, \dots, n\}$:

$$- \eta'_j - \sum_{i \neq j} \eta'_i \langle e_j^*, \varphi'_i \rangle + \langle e_j^*, w_t \rangle = \langle e_j^*, L[u] \rangle. \tag{39}$$

First, since $\frac{d}{dt} \langle e_j^*, w \rangle = 0$, it follows that $\langle e_j^*, w_t \rangle = \eta'_j \Lambda \int_{\mathbb{R}} e^{c(z-\eta_j)} w(z) \varphi''_j(z) dz$. The system for the positions $\eta = (\eta_1, \dots, \eta_n)^T$ is therefore given by $A\eta = \beta$, where $\beta_j = \langle e_j^*, L[u] \rangle$ and the matrix $A = (a_{i,j})$ is given by

$$a_{i,i} = -1 + \Lambda \int_{\mathbb{R}} e^{c(z-\eta_j)} w(z) \varphi''_j(z) dz$$

$$a_{i,j} = \langle e_j^*, \varphi'_i \rangle \text{ for } i \neq j.$$

Notice that if $i \neq j$, $a_{i,j} = O(e^{-\mu\delta_{\min}})$ and that $a_{i,i} = -1 + O(\|w\|)$, therefore in the expected asymptotics the matrix A is nearly equal to $-I_n$. The reduced ODE for the positions becomes

$$- \eta'_j(t) = \langle e_j^*(t), L[u(t)] \rangle + \text{hot}, \tag{40}$$

where the higher order terms hot are of order $\|w\|_{H^2(\mathbb{R})} + e^{-\mu\delta_{\min}} \sum \eta'_i$. In the following, we explain how this reduced ODE (40) leads to (17). For the sake of simplicity, during our computation we will include any other negligible terms into ‘hot’, without changing its name, keeping in mind the leading order we are interested in. We also focus on the (most intricate)

situation $1 < j < n$, the two specific cases $j = 1$ and $j = n$ being similar. Let us first notice that from (8),

$$\begin{aligned} L[u] &= \sum_{i=1}^n (\varphi_i'' + c\varphi_i') + w_{zz} + cw_z + f\left(\sum_{i=1}^n \varphi_i + w\right) \\ &= f\left(\sum_{i=1}^n \varphi_i\right) - \sum_{i=1}^n f(\varphi_i) + O(\|w\|_{W^{2,\infty}(\mathbb{R})}) \end{aligned}$$

so (40) becomes

$$-\eta_j'(t) = \left\langle e_j^*, f\left(\sum_{i=1}^n \varphi_i\right) - \sum_{i=1}^n f(\varphi_i) \right\rangle + \text{hot.} \tag{41}$$

The above bracket is an integral over \mathbb{R} (see (36)). Let us fix M large enough, such that $0 < M < \delta_{\min}$, to be determined later. We split the integration over three domains

$$\mathbb{R} = (-\infty, \eta_{j+1} + M] \cup [\eta_{j+1} + M, \eta_{j-1} - M] \cup [\eta_{j-1} - M, \infty),$$

so that

$$-\eta_j'(t) = I_1^- + I_2 + I_1^+ + \text{hot.} \tag{42}$$

Leading order terms: integration around the front Let us first focus on I_2 , since it is the most important term. Notice that for $z \in [\eta_{j+1} + M, \eta_{j-1} - M]$ one has, from (34) and classical invariant manifold theory that

$$\begin{cases} \varphi_i(z) = a_+ e^{\lambda(z-\eta_j)} + \text{hot}, & \text{for } i > j \\ 2\pi - \varphi_i(z) = a_- e^{\mu(z-\eta_i)} + \text{hot}, & \text{for } i < j, \end{cases} \tag{43}$$

and that their derivatives satisfy similar estimates. Then, using the 2π -periodicity of f , and linearizing at φ_j and 0, one has (see also (51) and (52)):

$$\begin{aligned} \frac{1}{\Lambda} I_2 &= \int_{\eta_{j+1}+M}^{\eta_{j-1}-M} e_j^*(z) \left(f\left(\sum_{i=1}^n \varphi_i(z)\right) - \sum_{i=1}^n f(\varphi_i(z)) \right) dz \\ &= \int_{\eta_{j+1}+M}^{\eta_{j-1}-M} e_j^* \left(f\left(\varphi_j + \sum_{i<j} (\varphi_i - 2\pi) + \sum_{i>j} \varphi_i\right) - f(\varphi_j) \right. \\ &\quad \left. - \sum_{i<j} f(\varphi_i - 2\pi) - \sum_{i>j} f(\varphi_i) \right) dz \\ &= \int_{\eta_{j+1}+M}^{\eta_{j-1}-M} e_j^*(z) (f'(\varphi_j(z)) - f'(0)) \left(\sum_{i<j} (\varphi_i(z) - 2\pi) + \sum_{i>j} \varphi_i(z) \right) dz + \text{hot} \end{aligned} \tag{44}$$

where the higher order terms in (44) are of order $\text{hot} = O((\delta_j + \delta_{j-1})e^{-2\mu M})$ as can be seen by (43). We split the integral in (44) between the left interacting fronts ($i > j$) and the right interacting fronts ($i < j$). Once again, the leading order terms are determined by the closest fronts, φ_{j+1} and φ_{j-1} respectively. It follows that

$$\frac{1}{\Lambda} I_2 = \int_{\eta_{j+1}+M}^{\eta_{j-1}-M} e_j^*(z) (f'(\varphi_j(z)) - f'(0)) (\varphi_{j-1}(z) - 2\pi) dz$$

$$\begin{aligned}
 & + \int_{\eta_{j+1}+M}^{\eta_{j+1}-M} e_j^*(z) (f'(\varphi_j(z)) - f'(0)) (\varphi_{j+1}(z)) dz + \text{hot} \\
 I_2 & = I_2^R + I_2^L + \text{hot}.
 \end{aligned}$$

From (43) and the definition of e_j^* , we infer that

$$\begin{aligned}
 I_2^L & = e^{\lambda(\eta_j - \eta_{j+1})} \Lambda a_+ \int_{\mathbb{R}} e^*(z) (f'(\varphi(z)) - f'(0)) e^{\lambda z} dz + \text{hot} \\
 & = -a_L e^{\lambda(\eta_j - \eta_{j+1})} + \text{hot},
 \end{aligned} \tag{45}$$

$$\begin{aligned}
 I_2^R & = -e^{\mu(\eta_j - \eta_{j-1})} \Lambda a_- \int_{\mathbb{R}} e^*(z) (f'(\varphi(z)) - f'(0)) e^{\mu z} dz + \text{hot} \\
 & = a_R e^{\mu(\eta_j - \eta_{j-1})} + \text{hot},
 \end{aligned} \tag{46}$$

where the coefficients a_L, a_R are precisely those given in (17). To complete our derivation of (17) it remains to determine the sign of these coefficients. We present the computation for a_L , the case a_R being similar. It uses estimates (34) for φ and its derivatives up to order 2, as well as the observation that $\varphi' f'(\varphi) = -\varphi''' - c\varphi''$. It follows that

$$\begin{aligned}
 a_L & = -\Lambda a_+ \int_{\mathbb{R}} e^{cz} \varphi'(z) (f'(\varphi(z)) - f'(0)) e^{\lambda z} dz \\
 & = -\Lambda a_+ \int_{\mathbb{R}} e^{-\mu z} (-\varphi'''(z) - c\varphi''(z) - f'(0)\varphi'(z)) dz
 \end{aligned} \tag{47}$$

$$= \Lambda a_+ \left(2\mu^2 a_- + c\mu a_- + (\mu^2 + c\mu + f'(0)) \int_{\mathbb{R}} e^{-\mu z} \varphi'(z) dz \right) \tag{48}$$

with three successive integration by parts from (47) to (48). Finally, notice that $\mu^2 + c\mu + f'(0) = 0$, and one gets

$$a_L = \Lambda a_+ a_- \mu (2\mu + c) > 0. \tag{49}$$

A quite similar computation gives

$$a_R = \Lambda a_+ a_- \lambda (2\lambda + c) > 0 \tag{50}$$

Negligible terms: integration away from the front It remains to prove that the integral I_2 is actually the one that drives the dynamics, and to discuss which value of M would be appropriate. We focus on I_1^- for the computations, the situation being similar for I_1^+ . Let us first notice that linearizing at any front, we obtain that for all $z \in \mathbb{R}$,

$$f \left(\sum_{i=1}^n \varphi_i(z) \right) - \sum_{i=1}^n f(\varphi_i(z)) = O \left(e^{-\frac{\mu}{2} \delta_{\min}} \right), \tag{51}$$

while, linearizing around at φ_{j+1} , we have that for all $z \in [\eta_{j+1}, \eta_{j+1} + M]$,

$$f \left(\sum_{i=1}^n \varphi_i(z) \right) - \sum_{i=1}^n f(\varphi_i(z)) = O \left(e^{\mu(z - \eta_j)} + e^{\lambda(z - \eta_{j-2})} \right). \tag{52}$$

Then, once again we split the integration domain into two.

$$\frac{1}{A} I_1^- = \int_{-\infty}^{\eta_{j+1}+M} e_j^*(z) \left(f \left(\sum_{i=1}^n \varphi_i(z) \right) - \sum_{i=1}^n f(\varphi_i(z)) \right) dz$$

$$\begin{aligned}
 &= \int_{-\infty}^{\eta_{j+1}} e_j^* \left(f \left(\sum_{i=1}^n \varphi_i \right) - \sum_{i=1}^n f(\varphi_i) \right) dz + \int_{\eta_{j+1}}^{\eta_{j+1}+M} e_j^* \left(f \left(\sum_{i=1}^n \varphi_i \right) - \sum_{i=1}^n f(\varphi_i) \right) dz \\
 &= J_1 + J_2.
 \end{aligned}$$

Combining (51), (34) and the definition of e_j^* , we get that

$$\begin{aligned}
 J_1 &= \int_{-\infty}^{\eta_{j+1}} e^{c(z-\eta_j)} \varphi'(z-\eta_j) f \left(\sum_{i=1}^n \varphi_i(z) \right) - \sum_{i=1}^n f(\varphi_i(z)) dz \\
 |J_1| &\leq C \int_{-\infty}^{\eta_{j+1}} e^{c(z-\eta_j)} e^{\mu(z-\eta_j)} dz e^{-\frac{\lambda}{2} \delta_{\min}} \leq C e^{(\lambda-\mu/2)\delta_{\min}} \tag{53}
 \end{aligned}$$

for some positive constant C . On the other hand, using (52) and (34), one has that for some positive constant C , possibly distinct from the above one,

$$\begin{aligned}
 |J_2| &\leq C \int_{\eta_{j+1}}^{\eta_{j+1}+M} e^{-\lambda(z-\eta_j)} \left(e^{\mu(z-\eta_j)} + e^{\lambda(z-\eta_{j+2})} \right) dz \\
 &\leq C \left(e^{(-2\mu-c)(\delta_j-M)} + M e^{\lambda(\delta_j+\delta_{j-1})} \right) \leq C \left(e^{(-2\mu-c)(\delta_{\min}-M)} + M e^{2\lambda\delta_{\min}} \right). \tag{54}
 \end{aligned}$$

Combining (53) and (54), we get, for some positive constant C ,

$$|I_1^-| \leq C \left(e^{(\lambda-\mu/2)\delta_{\min}} + e^{(-2\mu-c)(\delta_{\min}-M)} + M e^{2\lambda\delta_{\min}} \right). \tag{55}$$

Similar computations give the following estimates, for some positive constant C ,

$$|I_1^+| \leq C \left(e^{-\frac{3}{2}\mu\delta_{\min}} + e^{(\lambda-\mu)(\delta_{\min}-M)} + M e^{-2\mu\delta_{\min}} \right). \tag{56}$$

It remains to choose M and determine $\alpha > 0$ such that both I_1^-, I_1^+ , and the higher order terms in (44) are of order $e^{-(\mu+\alpha)\delta_{\min}}$, as long as δ_{\min} is large enough. Let us fix $\alpha > 0$ small enough, and $\varepsilon = \frac{\alpha}{\mu}$: we fix $M = \left(\frac{1}{2} + \varepsilon \right) \delta_{\min}$, and the estimates are as required.

B Proof of Theorem 6 (local stability of E)

We write $\Sigma_n = \sum_{k=1}^n \Psi_k^3 - \sum_{k=1}^{n-1} \Psi_k \Psi_{k+1}^2$ so (27) becomes

$$\Psi'_j = \begin{cases} \Psi_1 \left(\Psi_1^3 - \Psi_1 - \Psi_1 \Psi_2^2 + \sum_{k=2}^n \Psi_k^3 - \sum_{k=2}^{n-1} \Psi_k \Psi_{k+1}^2 \right), & j = 1 \\ \Psi_j \left(\Psi_j^3 - \Psi_j + \Psi_{j-1} - \Psi_j \Psi_{j+1}^2 - \Psi_{j-1} \Psi_j^2 + \sum_{\substack{k=1, \\ k \neq j}}^n \Psi_k^3 - \sum_{\substack{k=1, \\ k \notin \{j-1, j\}}}^{n-1} \Psi_k \Psi_{k+1}^2 \right), & 2 \leq j \leq n-1 \\ \Psi_n \left(\Psi_n^3 - \Psi_n + \Psi_{n-1} - \Psi_{n-1} \Psi_n^2 + \sum_{k=1}^{n-1} \Psi_k^3 - \sum_{k=1}^{n-2} \Psi_k \Psi_{k+1}^2 \right), & j = n \end{cases}$$

In the following, χ_A denotes the characteristic function which is either 1 if condition A is satisfied or 0 otherwise. For instance, for given $i \in \mathbb{N}$, $\chi_{\{i=2\}} = 1$ if $i = 2$ and 0 otherwise.

The Jacobian $J := \left(\frac{\partial f_j}{\partial \psi_i} \right)_{1 \leq i, j \leq n}$ is then given by

$$\frac{\partial f_1}{\partial \psi_i} = \begin{cases} -2\Psi_1 + 4\Psi_1^3 - 2\Psi_1 \Psi_2^2 + \sum_{k=2}^n \Psi_k^3 - \sum_{k=2}^{n-1} \Psi_k \Psi_{k+1}^2, & i = 1 \\ 3\Psi_1 \Psi_i^2 - 2\chi_{\{i=2\}} \Psi_1^2 \Psi_2 - \Psi_1 \Psi_{i+1}^2 - 2\chi_{\{i>2\}} \Psi_1 \Psi_{i-1} \Psi_i, & 2 \leq i \leq n-1 \\ 3\Psi_1 \Psi_n^2 - 2\Psi_1 \Psi_{n-1} \Psi_n, & i = n \end{cases}$$

and, for $2 \leq j \leq n - 1$ and $1 \leq i \leq n$,

$$\frac{\partial f_j}{\partial \Psi_i} = \begin{cases} \Psi_{j-1} - 2\Psi_j + 4\Psi_j^3 - 2\Psi_j\Psi_{j+1}^2 - 3\Psi_{j-1}\Psi_j^2 + \sum_{\substack{k=1, \\ k \neq j}}^n \Psi_k^3 - \sum_{\substack{k=1, \\ k \notin \{j-1, j\}}}^{n-1} \Psi_k\Psi_{k+1}^2, & i = j \\ \Psi_j + 3\Psi_{j-1}^2\Psi_j - \Psi_j^3 - 2\chi_{\{j>2\}}\Psi_{j-2}\Psi_{j-1}\Psi_j, & i = j - 1 \\ 3\Psi_j\Psi_{j+1}^2 - 2\Psi_j^2\Psi_{j+1} - \Psi_j\Psi_{j+2}^2, & i = j + 1 < n \\ 3\Psi_{n-1}\Psi_n^2 - 2\Psi_{n-1}^2\Psi_n, & i = j + 1 = n \\ 3\Psi_j\Psi_i^2 - \Psi_j\Psi_{i+1}^2 - 2\chi_{\{i>1\}}\Psi_j\Psi_{i-1}\Psi_i, & 1 \leq i \leq j - 2 \\ 3\Psi_j\Psi_i^2 - 2\Psi_j\Psi_{i-1}\Psi_i - \chi_{\{i < n\}}\Psi_j\Psi_{i+1}^2, & j + 2 \leq i \leq n \end{cases}$$

Finally, for $j = n$ and $1 \leq i \leq n$,

$$\frac{\partial f_n}{\partial \Psi_i} = \begin{cases} 4\Psi_n^3 - 2\Psi_n + \Psi_{n-1} - 3\Psi_{n-1}\Psi_n^2 + \sum_{k=1}^{n-1} \Psi_k^3 - \sum_{k=1}^{n-2} \Psi_k\Psi_{k+1}^2, & i = n \\ \Psi_n - \Psi_n^3 + 3\Psi_{n-1}\Psi_n^2 - 2\Psi_{n-2}\Psi_{n-1}\Psi_n, & i = n - 1 \\ 3\Psi_n\Psi_i^2 - \Psi_n\Psi_{i+1}^2 - 2\chi_{\{i>1\}}\Psi_n\Psi_{i-1}\Psi_i, & \text{else} \end{cases}$$

It remains to determine the eigenvalues of $J(E)$. To this end, since n is fixed throughout, we set $b := n(n + 1)(2n + 1) = 2n^3 + 3n^2 + n$ and $\beta = \frac{b}{6}$, $\alpha := \sqrt{1/\beta}$. Then $\alpha = \sqrt{\frac{6}{n(n+1)(2n+1)}}$ so that $E = \alpha(1, 2, \dots, n)^T$. After some straightforward computations, the first and last row of $J(E)$ are given by

$$\frac{\partial f_1}{\partial \Psi_i}(E) = \alpha^3 \cdot \begin{cases} -\beta - 1, & i = 1 \\ -1, & 2 \leq i \leq n - 1 \\ n^2 + 2n, & i = n \end{cases} \quad \frac{\partial f_n}{\partial \Psi_i}(E) = \alpha^3 \cdot \begin{cases} n(n^2 + 2n - \beta), & i = n \\ n(\beta - 1), & i = n - 1 \\ -n, & \text{else} \end{cases}$$

For $2 \leq j \leq n - 1$ and $1 \leq i \leq n$, the entries are

$$\frac{\partial f_j}{\partial \Psi_i}(E) = \alpha^3 \cdot \begin{cases} -j(1 + \beta(n)), & i = j \\ j(\beta(n) - 1), & i = j - 1 \\ -j, & i = j + 1 < n \\ n^3 + n^2 - 2n, & i = j + 1 = n \\ -j, & 1 \leq i \leq j - 2 \\ jn(n + 2), & j + 2 \leq i = n \\ -j, & j + 2 \leq i < n \end{cases}$$

Let $C := \{c_1, c_2, \dots, c_n\} := \alpha^{-3}J(E)$, where c_i are the column vectors. First note that the radial direction from E , $v_1 := (1, 2, 3, \dots, n)^T$, is an eigenvector of C with eigenvalue $\lambda_1 := 2\beta > 0$. However, this unstable direction is transverse to the invariant sphere and thus irrelevant here. Also by invariance, all remaining eigenvectors are orthogonal to v_1 .

A basis of the orthogonal complement $(\text{span}(v_1))^\perp$ is given by

$$V := \{v_2, v_3, \dots, v_n\}, \quad v_j := (j, 0, \dots, 0, -1, 0, \dots, 0)^T, \quad j = 2, \dots, n - 1,$$

where the entry -1 in v_j is on the j -th position. In order to reduce the matrix C onto the tangential dynamics, we orthogonalize the vectors v_j , $j = 1, 2, \dots, n$ by Gram-Schmidt and normalize afterwards. This results in the column vectors of the matrix W given by

$$w_1 := q_1 v_1, \quad w_k := q_k(1, 2, \dots, k - 1, -a_k, 0, \dots, 0)^T, \quad k = 2, 3, \dots, n,$$

with $a_k := \frac{1}{k} \sum_{i=1}^{k-1} i^2 = \frac{1}{6}(k - 1)(2k - 1)$ and normalizing constants

$$q_1 := \left(\sum_{i=1}^n i^2 \right)^{-1/2} = \frac{\sqrt{6}}{\sqrt{n(n+1)(2n+1)}}, \quad q_k := \left(\sum_{i=1}^k i^2 + a_k^2 \right)^{-1/2} = \frac{6}{\sqrt{4k^4 - 5k^2 + 1}}.$$

We claim that changing the basis with W yields the lower triangular matrix

$$W^T C W = \begin{pmatrix} \lambda_1 & 0 & 0 & \dots & 0 \\ 0 & b_{2,2} & 0 & \dots & 0 \\ 0 & b_{3,2} & b_{3,3} & \dots & 0 \\ \vdots & \vdots & \vdots & \ddots & \vdots \\ 0 & b_{n,2} & b_{n,3} & \dots & b_{n,n} \end{pmatrix}$$

with diagonal entries

$$b_{k,k} = -k\beta = -\frac{k}{6}n(n+1)(2n+1) < 0.$$

In order to prove this, we first note that with

$$d_k := (w_k \cdot c_1, w_k \cdot c_2, \dots, w_k \cdot c_n)^T$$

we have $b_{k,k} = d_k \cdot w_k$ so it remains to determine d_k for each $k \in \{2, 3, \dots, n\}$.

For $2 \leq k \leq n - 1$ and $1 \leq j \leq n - 1$,

$$w_k \cdot c_j = \begin{cases} -q_k \sum_{i=1}^{k-1} i^2 + ka_k q_k, & k < j \\ -q_k \sum_{i=1}^{k-1} i^2 + ka_k q_k (1 + \beta), & k = j \\ -q_k \sum_{i=1}^{j-1} i^2 - j^2 q_k (1 + \beta) - ka_k q_k (\beta - 1), & k = j + 1 \\ -q_k \sum_{\substack{1 \leq i \leq k-1, \\ i \notin \{j, j+1\}}} i^2 - j^2 q_k (1 + \beta) + ka_k q_k + (j + 1)^2 q_k (\beta - 1), & k \geq j + 2 \end{cases}$$

For $2 \leq k \leq n - 1$, we have $w_k \cdot c_n = q_k n(n + 2) \left(\sum_{i=1}^{k-1} i^2 - ka_k \right)$; finally, for $j < n$,

$$w_k \cdot c_j = -q_n \left(\sum_{\substack{1 \leq i \leq n-1, \\ i \notin \{j, j+1\}}} i^2 + j(1 + \beta) - (j + 1)^2 (\beta - 1) + a_n n(n^2 + 2n - \beta) \right)$$

and $w_n \cdot c_n = q_n \left(n(n + 2) \sum_{i=1}^{n-1} i^2 - a_n n(n^2 + 2n - \beta) \right)$.

This leads to the form $b_{k,k} = A_1 + A_2 + A_3$ with (after straightforward computations)

$$\begin{aligned} A_1 &:= \sum_{j=1}^{k-2} \left[j q_k^2 \left(ka_k + (j + 1)^2 (\beta - 1) - j^2 (1 + \beta) - \sum_{\substack{1 \leq i \leq k-1, \\ i \notin \{j, j+1\}}} i^2 \right) \right] \\ &= \left(\frac{3}{2k - 1} + \frac{42}{k + 1} - \frac{75}{2k + 1} \right) \beta, \\ A_2 &:= -(k - 1) q_k^2 \left(\sum_{i=1}^{k-2} i^2 + (k - 1)^2 (1 + \beta) + ka_k (\beta - 1) \right) \\ &= \left(\frac{72}{2k + 1} - \frac{36}{k + 1} - \frac{3}{2k - 1} - 3 \right) \beta, \\ A_3 &:= a_k q_k^2 \sum_{i=1}^{k-1} i^2 - ka_k^2 q_k^2 (1 + \beta) = \left(\frac{3}{2k + 1} + 3 - k - \frac{6}{k + 1} \right) \beta, \end{aligned}$$

and thus $b_{k,k} = -k\beta$. We conclude that the eigenvalues of C are

$$\lambda_{1,2} = \pm 2\beta, \quad \lambda_k = -k\beta, \quad 3 \leq k \leq n.$$

and thus E is locally exponentially stable on S^{n-1} . \square

Implementation of the simulations

In this section, we briefly describe the numerical methods and software used in the illustrating figures. The software packages we use are JCASIM [23] for simulating cellular automata, PDE2PATH [30] for PDE simulation, continuation and bifurcation package, and MATHEMATICA.

The space-time plot of the Greenberg-Hastings cellular automaton (Fig. 1a) has been created with JCASIM via an adaption of the method `transition`, where we specify the transition from one generation of cell states to the next according to the Greenberg-Hastings rule for $e = 2$ excited and $r = 4$ refractory states.

The phase portraits on the spheres (Fig. 5) have been created with MATHEMATICA using the standard routines `ParametricNDSolveValue`, `ParametricPlot` and `ParametricPlot3D`, respectively.

For the simulations of the PDE (1) plotted in 1b, Figs. 4, 8 and 9, we have used PDE2PATH with $f_0 = 0.05$ or $f_0 = 0.2$, respectively. As discretization of the interval $(-1x, 1x)$ by mesh width $2 * 1x / \text{dsc}$ we have chosen $1x=10$ and $\text{dsc}=500$ which corresponds to a mesh width of $h = 0.04$. Initial data `p.u(1:p.nu)` have been step functions with equilibrium levels at $e_{q+2} * \pi * j$ for $j = 1, 2, \dots, k, k \in \mathbb{N}$.

For the time stepping the PDE2PATH routines `tints` or `tintsfreeze` have been used since most simulations go over a rather long time period in order to catch exponentially small interaction effects between kinks (antikinks). `tintsfreeze` removes the translational symmetry so that the required spatial interval need not be excessively long. In particular, since annihilations of kinks and antikinks on the one side and interactions of kinks (antikinks) on the other side happen at different time scales (the annihilations being much faster), it is nearly impossible to observe both aspects simultaneously (even when choosing very large distances or a large space interval). We have circumvented this problem in Fig. 8 by starting with pure kink data “sending in” antikinks from the left space boundary repeatedly after time has allowed for observable exponentially small effects between the kinks that are left after each annihilation. This has been done by calling `tintsfreeze` multiple times and using the perturbed result as initial condition for the next call.

The detection of the kink (antikink) positions has been done via a function that stores the (geometrically defined) positions for each time step. The differences between these positions are the basis for the distance plots in Figs. 4, 8 and 9. For better illustration we have smoothed the distance plots by averaging the data and interpolating by splines using the MATLAB routine `interp1`. Finally, for general information about PDE2PATH and, in particular, the simulation with periodic boundary conditions (Fig. 9), we refer to [15] and the PDE2PATH webpage, respectively.

References

1. Angenent, S.B., Fiedler, B.: The dynamics of rotating waves in scalar reaction diffusion equations. *Trans. Am. Math. Soc.* **307**(2), 545–568 (1988)

2. Aranson, I.S., Kramer, L.: The world of the complex Ginzburg-Landau equation. *Rev. Modern Phys.* **74**(1), 99–143 (2002)
3. Adler, R.L., Konheim, A.G., McAndrew, M.H.: Topological entropy. *Trans. Am. Math. Soc.* **114**(2), 309–319 (1965)
4. Angenent, S.: The zero set of a solution of a parabolic equation. *J. Reine Angew. Math* **390**, 79–96 (1988)
5. Berestycki, H., Nirenberg, L.: On the method of moving planes and the sliding method. *Boletim da Sociedade Brasileira de Matemática - Bulletin/Brazilian Mathematical Society* **22**(1), 1–37 (1991)
6. Berestycki, H., Nirenberg, L.: Travelling fronts in cylinders. *Non-linear Anal.* **9**(5), 497–572 (1992)
7. Bowen, R.: Entropy for group endomorphisms and homogeneous spaces. *Trans. Am. Math. Soc.* **153**, 401–414 (1971)
8. Bellay, J., Scheel, A.: Coherent structures near the boundary between excitable and oscillatory media. *Dyn. Syst. Int. J.* **25**, 03 (2010)
9. Beyn, W.-J., Selle, S., Thümmler, V.: Freezing multipulses and multifronts. *SIAM J. Appl. Dyn. Syst.* **7**(2), 577–608 (2008)
10. Carr, J., Pego, R.L.: Metastable patterns in solutions of $u_t = \varepsilon^2 u_{xx} - f(u)$. *Commun. Pure Appl. Math.* **42**(5), 523–576 (1989)
11. Carter, P., Rademacher, J.D.M., Sandsted, B.: Pulse replication and accumulation of eigenvalues, accepted at *SIAM J Math. Ana.* (2021)
12. Chen, X.-Y., Matano, H.: Convergence, asymptotic periodicity, and finite-point blow-up in one-dimensional semilinear heat equations. *J. Differ. Equ.* **78**(1), 160–190 (1989)
13. Chen, H., Garcia-Gonzalez, D., Jérusalem, A.: Computational model of the mechanoelectrophysiological coupling in axons with application to neuromodulation. *Phys. Rev. E* **99**(3), 032406 (2019)
14. Ducrot, A., Giletti, T., Matano, H.: Existence and convergence to a propagating terrace in one-dimensional reaction-diffusion equations. *Trans. Amer. Math. Soc.* **366**(10), 5541–5566 (2014)
15. Dohnal, T., Rademacher, J. D. M., Uecker, H., Wetzel, D.: *pde2path 2.0: multi-parameter continuation and periodic domains*. In H. Ecker, A. Steindl, and S. Jakubek, editors, *ENOC 2014 - Proceedings of 8th European Nonlinear Dynamics Conference*. Institute of Mechanics and Mechatronics, Vienna University of Technology, (2014)
16. Durrett, R., Steif, J.E.: Some rigorous results for the Greenberg-Hastings model. *J. Theoret. Probab.* **4**(4), 669–690 (1991)
17. Ei, S.-I.: The motion of weakly interacting pulses in reaction-diffusion systems. *J. Dyn. Differ. Equ.* **14**, 85–137 (2002)
18. Fusco, G., Hale, J.K.: Slow-motion manifolds, dormant instability, and singular perturbations. *J. Dyn. Differ. Equ.* **1**(1), 75–94 (1989)
19. FitzHugh, R.: Impulses and physiological states in theoretical models of nerve membrane. *Biophys. J.* **1**(6), 445 (1961)
20. FitzHugh, R.: Computation of impulse initiation and saltatory conduction in a myelinated nerve fiber. *Biophys. J.* **2**(1), 11–21 (1962)
21. Fife, P.C., McLeod, J.B.: The approach of solutions of nonlinear diffusion equations to travelling front solutions. *Arch. Ration. Mech. Anal.* **65**(4), 335–361 (1977)
22. Fiedler, B., Mallet-Paret, J.: A Poincaré-Bendixson theorem for scalar reaction diffusion equations. *Arch. Ration. Mech. Anal.* **107**(4), 325–345 (1989)
23. Freiwald, U., Weimar, J.: *JCAsim—a Java System for Simulating Cellular Automata*, pp 47–54, 01 (2000)
24. Goh, R., Scheel, A.: Triggered fronts in the complex Ginzburg Landau equation. *J. Nonlinear Sci.* **24**, 117–144 (2014)
25. Greenberg, J.M., Hastings, S.P.: Spatial patterns for discrete models of diffusion in excitable media. *SIAM J. Appl. Math.* **34**(3), 515–523 (1978)
26. Greenberg, J.M., Hassard, B.D., Hastings, S.P.: Pattern formation and periodic structures in systems modeled by reaction-diffusion equations. *Bull. Amer. Math. Soc* **84**(6), 1296–1327 (1978)
27. Hodgkin, A.L., Huxley, A.F.: A quantitative description of membrane current and its application to conduction and excitation in nerve. *J. Physiol.* **117**(4), 500 (1952)
28. Hayase, Y., Ohta, T.: Self-replicating pulses and Sierpinski gaskets in excitable media. *Phys. Rev. E* **62**(5), 5998 (2000)
29. Hirsch, M.W., Pugh, C.C., Shub, M.: *Invariant manifolds*. Lecture Notes in Mathematics, vol. 583. Springer, Berlin (1977)
30. Wetzel, D., Uecker, H., Rademacher, J.D.M.: *pde2path: a matlab package for continuation and bifurcation in 2d elliptic systems*. *Numer. Math. Theory Methods Appl.* **7**(1), 58–106 (2014)
31. Kesseböhmer, M., Rademacher, J.D.M., Ulbrich, D.: Dynamics and topological entropy of 1D Greenberg-Hastings cellular automata. *Ergodic Theory Dyn. Syst.* **41**(5), 1397–1430 (2021)

32. Kuehn, C.: A remark on geometric desingularization of a non-hyperbolic point using hyperbolic space. *J. Phys. Conf. Ser.* **727**, 012008 (2016)
33. Lin, X.-B., Schechter, S.: Stability of concatenated traveling waves: alternate approaches. *J. Differ. Equ.* **259**(7), 3144–3177 (2015)
34. Ladyženskaja, O. A., Solonnikov, V. A., Ural'ceva, N. N.: *Linear and quasilinear equations of parabolic type*. Translated from the Russian by S. Smith. Translations of Mathematical Monographs, Vol. 23. American Mathematical Society, Providence, R.I., (1968)
35. Matano, H.: Asymptotic behavior of solutions of semilinear heat equations on S^1 . In W.-M. Ni, L. A. Peletier, and J. Serrin, editors, *Nonlinear Diffusion Equations and Their Equilibrium States II*, pages 139–162, New York, NY, (1988). Springer US
36. Matano, H., Poláčik, P.: Dynamics of nonnegative solutions of one-dimensional reaction-diffusion equations with localized initial data. Part II: Generic nonlinearities. *Commun. Partial Differ. Equ.* **45**(6), 483–524 (2020)
37. Nagumo, J., Arimoto, S., Yoshizawa, S.: An active pulse transmission line simulating nerve axon. *Proc. IRE* **50**(10), 2061–2070 (1962)
38. Nishiura, Y., Ueyama, D.: Self-replication, self-destruction, and spatio-temporal chaos in the Gray-Scott model. *Phys. Rev. Lett.* **15**(3), 281 (2000)
39. Poláčik, P.: Propagating terraces and the dynamics of front-like solutions of reaction-diffusion equations on \mathbb{R} . *Mem. Amer. Math. Soc.*, 264(1278):v+87, (2020)
40. Pauthier, A., Poláčik, P.: Large-time behavior of solutions of parabolic equations on the real line with convergent initial data. *Nonlinearity* **31**(9), 4423–4441 (2018)
41. Rinzel, J., Ermentrout, B.: Analysis of neural excitability and oscillations. *Methods Neuronal Model.* 01 (1998)
42. Risler, E.: Global behaviour of bistable solutions for gradient systems in one unbounded spatial dimension. *preprint*, (2017)
43. Rossides, T., Lloyd, D.J.B., Zelik, S.: Computing interacting multi-fronts in one dimensional real Ginzburg Landau equations. *J. Sci. Comput.* **63**(3), 799–819 (2015)
44. Roquejoffre, J.-M.: Stability of travelling fronts in a model for flame propagation. II. Nonlinear stability. *Arch. Rational Mech. Anal.* **117**(2), 119–153 (1992)
45. Redheffer, R.M., Walter, W.: The total variation of solutions of parabolic differential equations and a maximum principle in unbounded domains. *Math. Ann.* **209**, 57–67 (1974)
46. Sattinger, D.H.: On the stability of waves of nonlinear parabolic systems. *Adv. Math.* **22**(3), 312–355 (1976)
47. Scheel, A., Wright, J.D.: Colliding dissipative pulses—the shooting manifold. *J. Differ. Equ.* **245**(1), 59–79 (2008)
48. Scheel, A., Wright, J.D.: Colliding dissipative pulses—the shooting manifold. *J. Differ. Equ.* **245**(1), 59–79 (2008)
49. Scholtes, S., Westdickenberg, M.G.: Metastability of the Cahn-Hilliard equation in one space dimension. *J. Differ. Equ.* **265**(4), 1528–1575 (2018)
50. Volpert, A. I., Volpert, V. A., Volpert, V. A.: *Traveling wave solutions of parabolic systems*, volume 140 of *Translations of Mathematical Monographs*. American Mathematical Society, Providence, RI, (1994). Translated from the Russian manuscript by James F. Heyda
51. Westdickenberg, M. G.: On the metastability of the 1-d Allen-Cahn equation. *J. Dyn. Differ. Equ.* (2020)
52. Wiggins, S.: Normally Hyperbolic Invariant Manifolds in Dynamical Systems. *Applied Mathematical Sciences*, Vol. 105. Springer, Berlin, 01 (1994)
53. Wright, J.D.: Separating dissipative pulses: the exit manifold. *J. Dyn. Differ. Equ.* **21**(2), 315–328 (2009)
54. Zelik, S., Mielke, A.: Multi-pulse evolution and space-time chaos in dissipative systems. *Mem. Amer. Math. Soc.* 198(925):97 (2009)